

# **Towards an optimum patch in composite patch repair by finite element method**

Bhanu Prakash M

A Dissertation Submitted to  
Indian Institute of Technology Hyderabad  
In Partial Fulfillment of the Requirements for  
The Degree of Master of Technology



भारतीय प्रौद्योगिकी संस्थान हैदराबाद  
Indian Institute of Technology Hyderabad

Department of Mechanical Engineering

September, 2011

## Declaration

I declare that this written submission represents my ideas in my own words, and where others' ideas or words have been included, I have adequately cited and referenced the original sources. I also declare that I have adhered to all principles of academic honesty and integrity and have not misrepresented or fabricated or falsified any idea/data/fact/source in my submission. I understand that any violation of the above will be a cause for disciplinary action by the Institute and can also evoke penal action from the sources that have thus not been properly cited, or from whom proper permission has not been taken when needed.

---

(Signature)

Bhanu Prakash M  
(Student Name)

ME09G005  
(Roll Number)

## Approval Sheet

This thesis entitled “Modeling of Fatigue Crack Growth in Composite Repair by Finite Element Method” by Bhanu Prakash M is approved for the degree of Master of Technology from IIT Hyderabad.

---

Dr. R. Prasanth Kumar, Asst. Professor, IIT Hyderabad  
Examiner

---

Dr. B. Venkatesham, Asst. Professor, IIT Hyderabad  
Examiner

---

Dr. M. Ramji, Asst. Professor, IIT Hyderabad  
Advisor

---

Dr. B. Umashankar, Asst. Professor, IIT Hyderabad  
Chairman

## **Acknowledgements**

I would like to express a deep sense of gratitude towards my guide Dr. M. Ramji for providing excellent guidance, encouragement and inspiration throughout the project work. Without his invaluable guidance, this work would never have been successful. I would like to thank PhD students Mrs. Shrilakshmi and Mr. Mohammad Kashfuddoja and my classmate Amit Kulkarni for helping and giving suggestions on modeling aspects. I would like to thank Guruprasath sir for guiding and giving valuable suggestions regarding paper writing and creating nice environment in optics lab. I would like to thank all the M.Tech 2009-2011 batch students for helping me when I required. Last but not least, I would like to thank the institute, mechanical engineering department, and head of the department. I would also like to thank all my classmates for their valuable suggestions and helpful discussions.

## Table of contents

ACKNOWLEDGEMENTS .....	iv
ABSTRACT .....	v
LIST OF TABLES .....	x
LIST OF FIGURES .....	xi
NOMENCLATURE .....	xv

### CHAPTER 1 INTRODUCTION AND LITERATURE REVIEW

1.1	Introduction.....	1
1.2	Literature Review .....	5
1.3	Scope and Motivation.....	6
1.4	Thesis Layout.....	7

### CHAPTER 2 FINITE ELEMENT MODELLONG OF COMPOSITE REPAIR

2.1	Introduction.....	8
2.2	Finite element modeling .....	9
2.3	Composite repair model .....	10
2.4	Finite Element Modeling.....	11
	2.4.1 Cracked panel model .....	11
	2.4.2 Modeling of patch and adhesive .....	15
	2.4.3 Assembly of composite repair model .....	16
2.5	Validation of results .....	16
2.3	Closure .....	19

### CHAPTER 3 MODELLING AND ANALYSIS OF DOUBLE SIDED COMPOSITE REPAIR

3.1	Introduction.....	20
3.2	Patch Material .....	22
3.3	Modeling.....	22
3.4	Results and Discussions .....	23
	3.4.1 Elliptical Patch shape .....	23
	3.4.1 Circular Patch shape.....	25
	3.4.1 Rectangular Patch shape.....	27
3.5	Area normalization .....	31
3.6	Closure .....	33

#### CHAPTER 4 MODELLING AND ANALYSIS OF SINGLE SIDED COMPOSITE REPAIR

4.1	Introduction.....	34
4.2	Patch Material .....	35
4.3	Single sided patch for different crack inclination angles using unidirectional laminates .....	36
4.4	Unbalanced Laminates.....	38
4.5	Unbalanced Laminates applies to 30 degree crack.....	39
4.6	Unbalanced Laminates applies to 45 degree crack.....	42
4.7	Unbalanced Laminates applies to 60 degree crack.....	45
4.8	Comparison of $[90_4]$ and $[0_290_2]$ applied to different mixed mode cracks .....	47
4.9	Transversely graded materials .....	48
4.10	Transversely graded materials applied to different mixed mode cracks .....	49
4.11	Closure .....	51

CHAPTER 5 CONCLUSIONS AND RECOMMENDATIONS FOR FUTURE WORK	52
REFERENCES .....	54
LIST OF PAPERS SUBMITTED ON THE BASIS OF THIS THESIS .....	56

## LIST OF TABLES

<b>Table</b>	<b>Title</b>	<b>Page</b>
2.1	Patch material and their material properties.....	13
2.2	Comparison of SIF at panel surface solved by analytical and numerical analysis.....	17
3.1	Different patch shapes and their areas .....	30



## LIST OF FIGURES

Figure	Title	Page
1.1	Schematic of (a) Single side patch repair (b) Double side patch repair.....	3
1.2	Application of patch repair to the wing of F-111 military aircraft [1] .....	3
2.1	The contour and outward normal drawn in calculation of $J$ -integral .....	9
2.2	(a) Two coincident nodes near the crack tip before loading and (b) Two nearest nodes near the crack tip after loading .....	10
2.3	Twenty noded brick element in brick and prism type with red dots indicating the nodes .....	11
2.4	The panel interface area for different patch shapes (a) Circle(b) ellipse (c) rectangle (d) octagon .....	13
2.5	(a) panel area geometry (b) before meshing (c) after meshing .....	14
2.6	The panel volume after meshing for (a) rectangular patch (b) circular patch.....	14
2.7	The 3D mesh for (a) circular adhesive (b) circular patch.....	15
2.8	Variation of SIF through thickness for an un-patched crack inclination angle of (a) 0 degree (b) 30 degree (c) 45 degree (d) 60 degree.....	18
2.9	Variation of $J/J_{\text{un-repaired}}$ for different patch orientations for a 1.5 mm thick patch given by reference [23] and present work .....	19
3.1	Geometry of panel with crack for double sided repair.....	21
3.2	Variation of SIF through the thickness for a double sided elliptical patch for 30 degree crack (a) $K_I$ (b) $K_{II}$ .....	23
3.3	Variation of SIF through the thickness for a double sided elliptical patch for 45 degree crack (a) $K_I$ (b) $K_{II}$ .....	24

3.4	Variation of SIF through the thickness for a double sided elliptical patch for 60 degree crack (a) $K_I$ (b) $K_{II}$ .....	24
3.5	Variation of SIF through the thickness for a double sided circular patch for 30 degree crack (a) $K_I$ (b) $K_{II}$ .....	26
3.6	Variation of SIF through the thickness for a double sided circular patch for 30 degree crack (a) $K_I$ (b) $K_{II}$ .....	26
3.7	Variation of SIF through the thickness for a double sided circular patch for 30 degree crack (a) $K_I$ (b) $K_{II}$ .....	27
3.8	Variation of SIF through the thickness for a double sided rectangular patch for 30 degree crack (a) $K_I$ (b) $K_{II}$ .....	28
3.9	Variation of SIF through the thickness for a double sided rectangular patch for 45 degree crack (a) $K_I$ (b) $K_{II}$ .....	28
3.10	Variation of SIF through the thickness for a double sided rectangular patch for 60 degree crack (a) $K_I$ (b) $K_{II}$ .....	29
3.11	Variation of SIF through the thickness for a double sided patch area of 706 mm <sup>2</sup> (a) $K_I$ (b) $K_{II}$ .....	31
3.12	Variation of SIF through the thickness for a double sided patch area of 800 mm <sup>2</sup> (a) $K_I$ (b) $K_{II}$ .....	32
3.13	Variation of SIF through the thickness for a double sided patch area of 981 mm <sup>2</sup> (a) $K_I$ (b) $K_{II}$ .....	32
4.1	Geometry of panel with crack for single sided repair.....	35
4.2	Variation of SIF through the thickness for a rectangular patch for 30 degree crack (a) $K_I$ (b) $K_{II}$ .....	37
4.3	Variation of SIF through the thickness for a rectangular patch for 45 degree crack (a) $K_I$ (b) $K_{II}$ .....	37
4.4	Variation of SIF through the thickness for a rectangular patch for 60 degree crack (a) $K_I$ (b) $K_{II}$ .....	38
4.5	Variation of SIF through a rectangular patch of size 28x25 mm <sup>2</sup> for 30 degree crack (a) $K_I$ (b) $K_{II}$ .....	40
4.6	Variation of SIF through a rectangular patch of size 30X25 mm <sup>2</sup> for 30 degree crack (a) $K_I$ (b) $K_{II}$ .....	40
4.7	Variation of SIF through a rectangular patch of size 32x25 mm <sup>2</sup> for 30 degree crack (a) $K_I$ (b) $K_{II}$ .....	41

4.8	Variation of SIF through a rectangular patch of size 35.36x25 mm <sup>2</sup> for 30 degree crack (a) $K_I$ (b) $K_{II}$ .....	41
4.9	Variation of SIF through a rectangular patch of size 28x25 mm <sup>2</sup> for 45 degree crack (a) $K_I$ (b) $K_{II}$ .....	43
4.10	Variation of SIF through a rectangular patch of size 30X25 mm <sup>2</sup> for 45 degree crack (a) $K_I$ (b) $K_{II}$ .....	43
4.11	Variation of SIF through a rectangular patch of size 32x25 mm <sup>2</sup> for 45 degree crack (a) $K_I$ (b) $K_{II}$ .....	44
4.12	Variation of SIF through a rectangular patch of size 35.36x25 mm <sup>2</sup> for 45 degree crack (a) $K_I$ (b) $K_{II}$ .....	44
4.13	Variation of SIF through a rectangular patch of size 30x25 mm <sup>2</sup> for 60 degree crack (a) $K_I$ (b) $K_{II}$ .....	45
4.14	Variation of SIF through a rectangular patch of size 32x25 mm <sup>2</sup> for 60 degree crack (a) $K_I$ (b) $K_{II}$ .....	46
4.15	Variation of SIF through a rectangular patch of size 28x25 mm <sup>2</sup> for 60 degree crack (a) $K_I$ (b) $K_{II}$ .....	46
4.16	Variation of SIF through a rectangular patch of size 35.36x25 mm <sup>2</sup> for 60 degree crack (a) $K_I$ (b) $K_{II}$ .....	47
4.17	Variation of SIF through the thickness for different crack inclination angles for rectangular patch of size 35.36x25 mm <sup>2</sup> for patch lay-up [90 <sub>4</sub> ] (a) $K_I$ (b) $K_{II}$ .....	48
4.18	Variation of SIF through the thickness for different crack inclination angles for rectangular patch of size 35.36x25 mm <sup>2</sup> for patch lay-up [0 <sub>2</sub> 90 <sub>2</sub> ] (a) $K_I$ (b) $K_{II}$ .....	48
4.19	Variation of E through thickness of patch.....	49
4.20	Variation of SIF through the thickness for a single sided rectangular patch for 30 degree crack (a) $K_I$ (b) $K_{II}$ .....	50
4.21	Variation of SIF through the thickness for a single sided rectangular patch for 45 degree crack (a) $K_I$ (b) $K_{II}$ .....	50
4.22	Variation of SIF through the thickness for a single sided rectangular patch for 60 degree crack (a) $K_I$ (b) $K_{II}$ .....	51

## Nomenclature

SIF	Stress Intensity Factor
FEM	Finite Element Method
FEA	Finite element analysis
$\theta$	Crack inclination angle
$\sigma$	Stress
$E$	Youngs Modulus
$\nu$	Poissons ratio
$K_I$	Stress Intensity Factor in mode-I
$K_{II}$	Stress Intensity Factor in mode-II
$J$	J-integral value
$\Delta u_x$	Difference of x component of nodal displacements of nodes nearest to crack tip
$\Delta u_y$	Difference of y component of nodal displacements of nodes nearest to crack tip



# Chapter 1

## Introduction and literature review

### 1.1 Introduction

All metallic structures are prone to degradation by cracking and corrosion in service, particularly when design, manufacture or environmental protection is inadequate to meet actual serviced usage. In military aircraft fatigue cracking may be more of a problem than originally envisaged because of exposure to more severe loads than originally anticipated. Because of limited budgets and escalating replacement costs, many military aircraft are being maintained in service well past their planned life [1]. Cracks can arise from repeated loading (fatigue). Fatigue cracks arise from highly localized cyclic plastic deformation caused by fluctuating service loads. These cracks pose the greatest threat to structural integrity since they grow perpendicularly to the applied load direction and eventually severing the load path [1].

Repairs based on mechanically fastened metallic patches compared to adhesively bonded patches are less efficient and more problem prone because of high stresses at the fasteners and fastener holes resulting in significant local displacements, therefore higher stress intensity factors (SIF). The main concern is the danger of initiation of a crack from a fastener hole. The crack may initiate at quite low stresses because of high stress concentrations because of poor quality hole drilling or riveting [1]. By contrast, loads in bonded joints are transferred by shear over the surface area of the elements. Because of the large area for load transfer, the bonded repair is much stiffer than the mechanical joint. Other advantages are it seals interfaces to reduce corrosion leakage and also it creates minimal damage to the parent structure. This has been used on

aircraft and ship structures, and on wind turbine blades. The approach of using adhesive bonding to repair or reinforce damaged aircraft structure has been shown to be a highly cost effective alternative to the conventional repair methods. Thousands of adhesively bonded repairs have now been applied to hundreds of aircraft in service with the Royal Australian Air Force (RAAF) and United States Air Force (USAF) since the middle 1970 [2].

The history of the aging aircraft program for the USAF began on 13 March 1958 with the structural fatigue failure of the wing of the B-47. Those events led directly to the initiation of the USAF Aircraft Structural Integrity Program (ASIP). The ASIP defines all of the structurally related activities on an aircraft from initial development until retirement; therefore, it can be considered an aging aircraft program. This program was significantly changed as a result of the failure of an F-111 on 22 December 1969 by elevating the technology basis of the program from fatigue to fracture [3].

In 1972 DSTO (Defense science and technology organisation) invented, and now leads the world in the use of composite bonded repairs to reinforce and repair aircraft structures. Originally developed to prolong the life of RAAF fighter aircraft, this invention has been applied to US Air Force aircraft as well as the civilian 727 and the 767. Continued research at DSTO in area of crack-patching pioneered by Alan Baker made DSTO world leader in this technology. Since then a large number of aircraft like MB-326H, Mirage III, C-130E, F-111C etc are repaired. While adhesive bonded repairs are a very effective means of managing structural issues, there are some circumstances where the use of adhesive bonded repairs would be inappropriate and limited. The load bearing capabilities of adhesive bonds depends directly on the properties of the adhesive, and these properties vary significantly with temperature [2].

Two kinds of patch work are employed in composite repair: first is single sided (un-symmetrical) and the second one is double sided (symmetrical patch). In case of single sided repair, bending effect in addition to in-plane tensile loading is there. These bending stresses severely effects the fracture parameter. In double sided repair two identical reinforcements are bonded on the two surfaces of a cracked plate. This

symmetric arrangement ensures that there is no out-of-plane bending over the repaired region provided the cracked plate is subjected to extensional loads only. Mostly double side patch work is preferred over single side. This is because the single-side repair introduces additional bending effect due to offset in neutral axis other than in-plane tensile load. Also there is bending due to different thermal coefficient of expansion between patch and panel. Although it has been shown that a symmetric repair is the most effective reinforcement, unsymmetric repairs provide a clear advantage when it is difficult or not possible to access both sides of a structure. (eg repair on wing surfaces).

Lot of experimental and numerical studies have been done in area of composite repair to understand the mechanics. Among the numerical methods, Finite element method is ideally preferred for its versatility and accuracy. Over last two decades, an enormous growth/understanding has been established in area of FEA (Finite element analysis) applied to fracture mechanics and especially in area of composite repair.

A detailed review of application of FEM (Finite element method) to composite repair is available in literature. But not much work exists in the literature in the area of optimisation of composite patch repair applied to mixed-loading. In this work the effect of patch shape is studied for a mixed-mode crack (Crack inclination angles of 30,45 and 60 degrees). Also for the same area, the effect of different shapes of patch is studied.

Bonded repairs function by transferring some portion of the load from the repair component to the patch through the adhesive bond layer, thereby increasing the static strength of the cracked panel. The relative stiffness of the reinforcement, as compared to the repaired component, determines not only the portion of load transferred, but also the level of peak stresses in the adhesive layer, and the intensity of associated stress concentrations in the repaired component. It is important to note that due to air safety considerations, when applied to primary structural components, bonded repairs are typically used as a measure to prevent crack initiation and retard crack growth [1]. It is generally required that the component has adequate static strength with or without the



bonded repair. Hence, in some cases it is necessary to restore residual static strength before the application of a bonded repair.

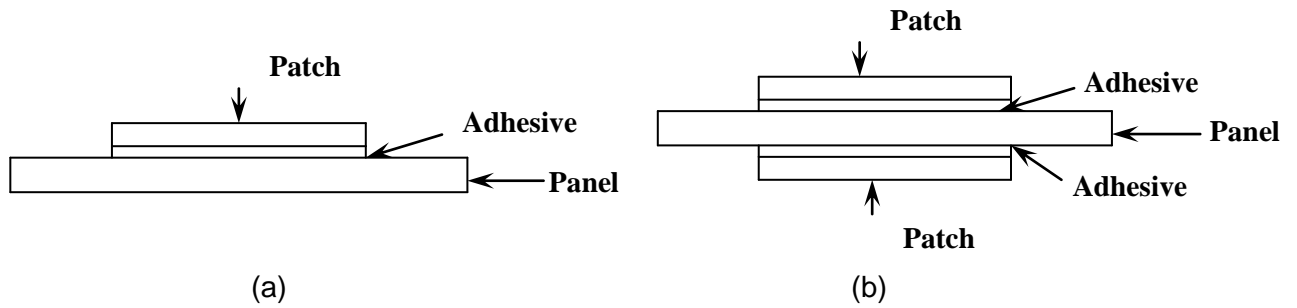


**Figure 1.1:** Schematic of (a) Single side patch repair (b) Double side patch repair

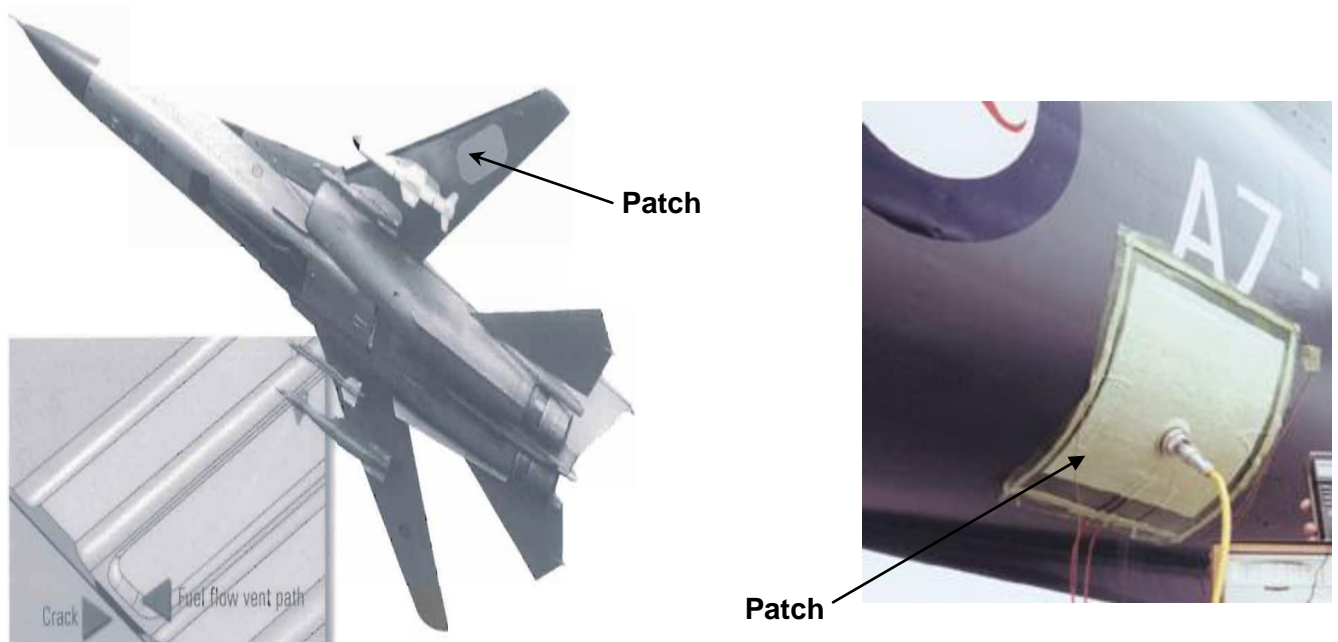


**Figure 1.2:** Application of patch repair to the wing of F-111 military aircraft [1]

## 1.2 Literature Review

The use of adhesively bonded repairs has been initiated by DSTO in 1970s. Study in this field involved both experimental and numerical methods. Significant work in literature is contributed by A A Baker [1]. In 1978, patching in military aircrafts utilizing boron fibre reinforced laminates are described which prevent or considerably reduce crack propagation due to fatigue in cracked aircraft component [4]. In 1980, numerical investigation into crack patching by Jones showed that a modified form of the crack opening displacement approach may be useful in estimating the effect that fiber composite patches have on cracks in thin sheets [5]. Further in 1983, a finite element method for analysis of cracks in thin fiber composite sheets which were repaired with a bonded overlay (boron/epoxy) [6]. In 1985, Ramesh Chandra analytically predicted the SIF double sided repaired panel [7]. In 1989, FE analysis of mixed mode symmetrically repaired crack was done by Sethuraman and Maiti [8]. After this they studied the effect of rectangular patches by study of effect of rectangular patches on cracks in mode I or mode II [9]. In 1994, Ching-Hwei studied the performance of the bonded repairs of a plate containing an inclined central crack under biaxial loading [10] and later Ching-Hwei studied the effect of laminated composite patch with different stacking sequences on repairing an inclined central cracked plate under biaxial loading [11]. In 1996, Tay carried out the single sided bonded repairs on aluminium panels with a cracked bolt hole using patches concluding that the composite patch greatly reduced the crack growth rate [12]. In 1997 Chorng-Fuh Liu calculated SIF of patched crack using numerical methods concluding that as the thickness of the patch increases, there would be significant differences between 2d and 3d repaired models [13]. Work on bending effects of unsymmetrical bonded repairs were studied by Klug [14], Scott [15] independently in 1998. Umamaheswar studied on the modeling aspects of bonded repaired panel to arrive at a correct procedure [16]. They further concluded that single brick along the thickness of panel, patch and adhesive was fairly sufficient to predict the fracture parameters accurately. In 2000 Mahadesh Kumar studied an optimum patch configuration for a center crack studying the effects of different patch shapes and different patch thickness [17]. In 2002, Bachir Bouiadjra showed that in mixed mode loading, the mode I stress intensity factor is more affected by the presence of the

patch than that of mode II [18]. In 2002, Dae-Cheol Seo showed that there exist large variations of SIF through the thickness of repaired panel [19]. In 2003, Wang studied the effect of number of plies in composite patch repair on fracture parameters concluding that 4-ply-patch repaired specimen demonstrated its effectiveness in preventing static failure and increasing fatigue life of the cracked substrates [20]. In 2003, Ki Hyun Chung showed that the maximum effectiveness of patch was obtained from the plate with  $0^\circ$  inclined crack and the effect was relatively small in  $30^\circ$  and  $45^\circ$  inclined crack [21]. In 2006, Jean-Denis Mathias used genetic algorithm for shape optimization of patch for a given overlap area varying the ply configuration and patch shape for a given patch area [22]. Toudeshky performed finite element analysis of mixed mode crack repair of aluminium panels using composite patch [23]. In 2007, Hosseini-Toudeshky studied mixed mode crack in thin aluminium panels repaired by composite patch and concluded that most life extension including the crack propagation cycles belongs to the patch lay-up of in which all fibres are oriented along the loading direction [24]. In 2008, K. Madani studied the effect of adhesive thickness for a mode I crack varying the adhesive thickness which concluded that when the thickness of adhesive increases, the SIF increased, however a minimum adhesive thickness is required [25].

In this work, the effect of the patch geometry on different mixed mode cracks ( crack inclination angle of  $30^\circ$ ,  $45^\circ$  and  $60^\circ$  degrees) is studied for both single and double sided repair. Further the effect of unbalanced laminates and transversely graded material is studied on single sided repair.

In the present work, we consider the panel dimensions as considered by Toudeshky [28] for a  $45^\circ$  degree centre crack and design the optimal patch for it and also for calculation of fracture parameters.

### **1.3 Scope and Motivation**

Most of the optimization work in composite patch repair deals with fracture in mode I and not much work exists in literature in patch shape optimization for mixed mode

crack. This project gives scope for designing the optimal patch for a given mixed mode crack. It is equally challenging to create the FE model for different patch shape geometries. In single sided repair there is bending in addition to in-plane load because of neutral axis shift. Thus its behavior is different from double sided model. For counteracting this bending effect unbalanced laminate is proposed. Later transversely graded patch material is also proposed for the first time in literature.

#### **1.4 Thesis Layout**

Chapter 1 mainly consists of the introduction to the fracture in aircraft panels, literature review, scope and objective of the dissertation

Chapter 2 deals with the finite element modeling of the cracked panel with and without repair

Chapter 3 describes the patch shape effect on double sided repair for different mixed mode conditions using unidirection composite patch of  $[90_4]$  patch layup

Chapter 4 describes the patch shape effect on single sided repair using composite reinforcement involving balanced laminate. Later unbalanced laminate and also transversely graded material is considered as an alternate patch material for alleviating the SIF at un-patched surface

Chapter 5 deals with the conclusions and recommendations for future work.

# CHAPTER 2

## Finite element modelling of composite repair

### 2.1 Introduction

Aircraft panels repaired by composite patches have to be designed efficiently. In this study, the effect of patch on a mixed mode crack is studied. Since inclined crack being a mixed-mode fracture, we must efficiently design a patch which can handle both the modes effectively. The study can be done experimentally, analytically or numerically. The experimental analysis carried out as industrial research because of the vast costs involved in the equipment (DIC-Digital image correlation and photoelasticity) and also preparing the specimen. Numerical analysis is done based on Finite element method (FEM). The cost involved in computation is less as compared to experimental investigation. Solving the partial differential equations of a discretized structure with finite number of small elements connected by nodes, is the governing principle behind the finite element method. For this, the meshing should be done with care and required boundary conditions need to be applied correctly. The first one being pre-processing, involves development of 2D or 3D models of the structure followed by the selection of materials and finally discretizing the entire domain into finite number of elements, also called as meshing. The second step is to develop and solve locally (at each element) the governing equations by converting it into linear set of algebraic equations. Subsequent evaluation of results in the visualization and measurement of deformation comes under post processing. In this work, commercially available code ANSYS to perform finite element analysis (FEA). ANSYS has been widely used by various organizations and its solver is generally reliable for getting accurate solutions in field of structural mechanics.

## 2.2 Fracture analysis of Three-Dimensional Models

Obtaining fracture parameters using FEM involves estimating the fracture parameter SIF in mode-I ( $K_I$ ) and mode-II ( $K_{II}$ ) through numerical integration.

Towards this, one needs to evaluate of J integral. The definition of J integral is given by J rice in 1968 [1] as shown below:

$$\oint_C [Wn_1 - \sigma_{ij}n_j \frac{\partial u_i}{\partial x}] ds \quad (2.1)$$

where  $W$  is strain-energy density;  $\sigma_{ij}$  are stress elements;  $u_i$  are the displacements corresponding to local  $n$ -axis;  $s$  is the arc length of the contour;  $n_j$  is the  $j^{\text{th}}$  component of the unit vector outward normal to the contour  $C$ , which is any path of vanishing radius surrounding the crack-tip. The contour and outward normal along the crack is shown in Figure 2.1.

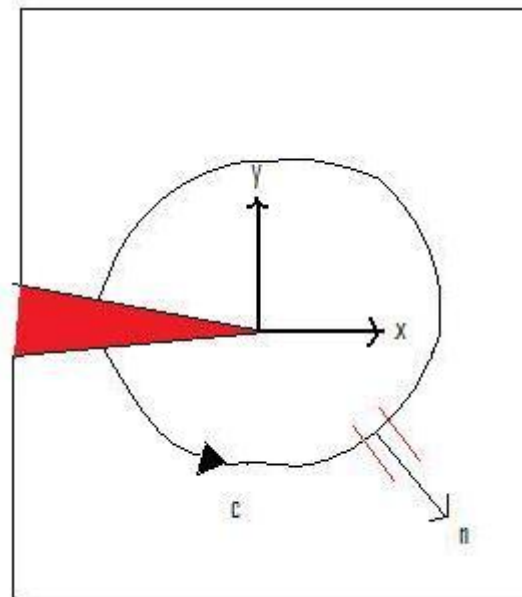


**Fig 2.1:** The countour and outward normal drawn along it in calculation of  $J$ -integral .

The value of  $J$ -integral is equal to the energy release rate ( $G$ ) in framework of linear elastic fracture mechanics (LEFM). After the initial formulation of the  $J$ -integral method by Rice [26], Shih et al. [27] modified the initial contour integral to an area integral in two dimensions and a volume integral in the three dimensional case. The  $J$ -Integral approach is preferred because it is well established in major FEM codes;

also it is robust and does not require intensive mesh refinement in the vicinity of the crack tip. Another popular method for calculating SIF is the use of quarter point elements (collapsed elements) in the crack tip vicinity. These elements capture the crack-tip singularity precisely. In ANSYS, there are elements which facilitate calculation of  $J$ -integral. In calculating  $K_I$  and  $K_{II}$  from the  $J$  value we use the following relations.

$$J = K_I^2/E' + K_{II}^2/E' \quad (2.2)$$

Where  $E' = E/(1 - \nu^2)$  which is relationship for plane strain case

It is assumed that the ratio of  $K_I$  over  $K_{II}$  is the ratio of normal distance of two closest nodes to the horizontal distance of the two closest nodes [23]. The nodal displacements of nodes nearest to crack tip are shown in Figure 2.2.

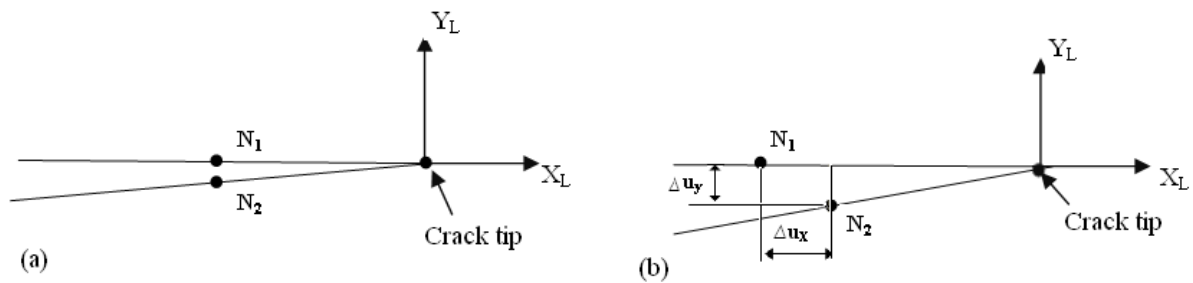


**Fig 2.2:** (a) Two coincident nodes near the crack tip before loading and (b) Two nearest nodes near the crack tip after loading.

### 2.3 Finite element modeling

The element used in this work is a 20 noded brick element with three degrees of freedom at each node as shown in Figure 2.3. These elements facilitate the calculation of  $J$ -integral value using CINT command which in turn uses the domain integral method for evaluation. It is sufficient to have two elements along the thickness of the panel. However to capture the bending stresses of the panel accurately which appears in place in single sided repair, six elements are kept along the panel thickness. The meshing around the crack-tip has to be done finely in order to capture the high stress gradient. Around the crack tip, 19 elements along radial direction are used and 36 elements along circumferential divisions are employed for the above said purpose. The mesh gets coarser as we move away from the crack

tips. The area on panel where patching is done, meshing is kept similar to that which will be done for patch and adhesive. For doing this, mapped meshing is carried out in these areas. This ensures that the nodes on the interface areas are coincident which needs to be coupled to mimic bonded behavior. Another method of gluing the interface areas is using the Multi point constraint algorithm (MPC). This algorithm takes the nodes of the interface areas as input and appropriately transfers the nodal displacements, force etc to the other set of nodes similar to that of glued areas. The advantage of MPC algorithm is that the patch and adhesive need not have similar mesh pattern similar to that of the panel therefore providing a greater flexibility. Comparatively, in  $J$ -integral values obtained using both methods are same.



**Fig 2.3** Twenty noded solid element in brick and prism type with red dots indicating the nodes

## 2.4 Composite Repair Model

### 2.4.1 Cracked Panel Model

The geometry of the panel, adhesive and patch is shown in the Figure 2.5. Aluminium sheet of dimension 170 mm x 39 mm x 3.175 mm, with an inclined center crack of length  $2a = 10$  mm is considered. Initially two dimensional area is created with the crack as per required geometry. For this at first the crack tip is created and around it a very fine meshed area is created as shown in Figure 2.5. This meshing is done using mesh 200 elements (8 noded). Mesh 200 elements do not have any



stiffness matrix associated with it. It facilitates sweeping the area mesh pattern to create finite 3D model. Then the adhesive interface area is created which includes these finely meshed areas. The patch area is of mapped meshed nature. Then we create the 2D meshed panel as shown. We can notice that after meshing there are two coincident nodes along the crack. To create the 3-D panel, the created area are extruded along the thickness direction (thickness = 3.175 mm from  $z = 0$  to  $z = -3.175$ ) to create the panel volume. All lines along the thickness are divided into six segments. Then all the area mesh is swept through the volume with solid 186 elements. After the panel is formed, the mesh 200 elements are deleted.

To calculate  $J$ -integral using CINT command, some inputs must be defined. These are the nodes through the crack tip, a coordinate system. First we define all the nodes through the crack tip. For this we create a component. A component is a set of areas, nodes, volumes, etc. These are user defined. The set of nodes through the crack tip is created as a component and it is named as "CRIGHT" for right crack tip and "CLEFT" for the left crack tip. A local coordinate system is to be created with the origin at crack tip and axis such that one is along the crack and the other perpendicular to the crack face. This local coordinate system and the nodes are the input for calculating  $J$  integral.

On the top face of the panel 121.11 MPa tensile pressure is applied and on the bottom face all degrees of freedom of all nodes are arrested. The pressure load 121.11 MPa corresponds to a load of 15 KN force acting in-plane. For coupling of nodes at interface surfaces, components of these nodes are formed. The nodes at interface area is named as "PANELNODES", nodes of the crack along the surface thickness is "CRACKNODES". The material properties of the repair elements is shown in Table 2.1. The patch is composite boron-expoy having orthotropic properties and panel and adhesive are isotropic.

**Table 2.1.** Patch material and their material properties

Material	$E_x$ (GPa)	$E_y$ (GPa)	$E_z$	$\nu_{xy}, \nu_{xz}$	$\nu_{yz}$	$G_{xy}$ (GPa)	$G_{xz}$	$G_{yz}$ (GPa)
Aluminium	71.02			0.3				
Adhesive-FM77	1.83			0.33				
Boron/epoxy	208.1	24.44		0.1677	0.035	7.24		4.94

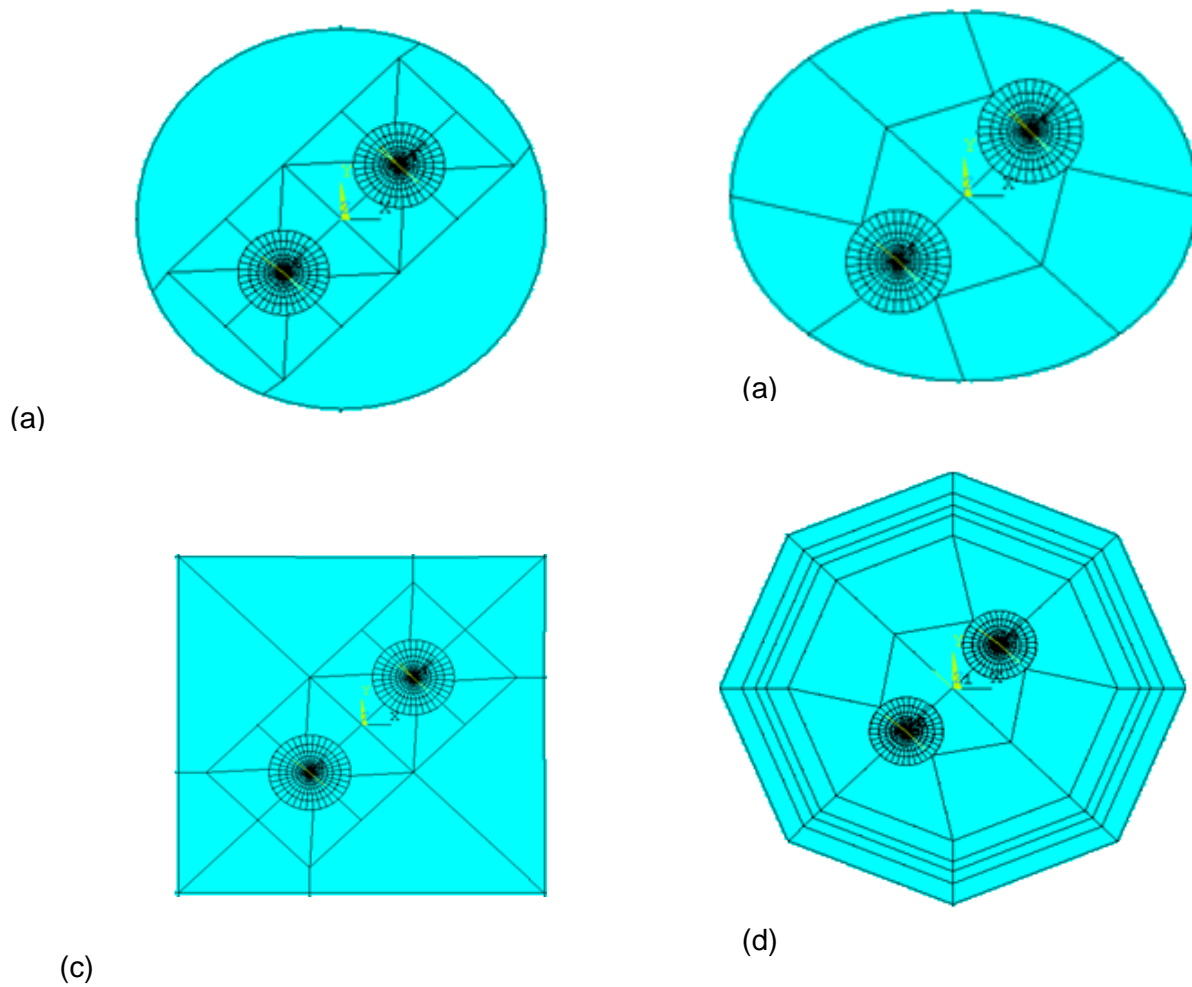


**Fig 2.4:** The panel interface area for different patch shapes (a) circle (b) ellipse (c) rectangle (d) octagon

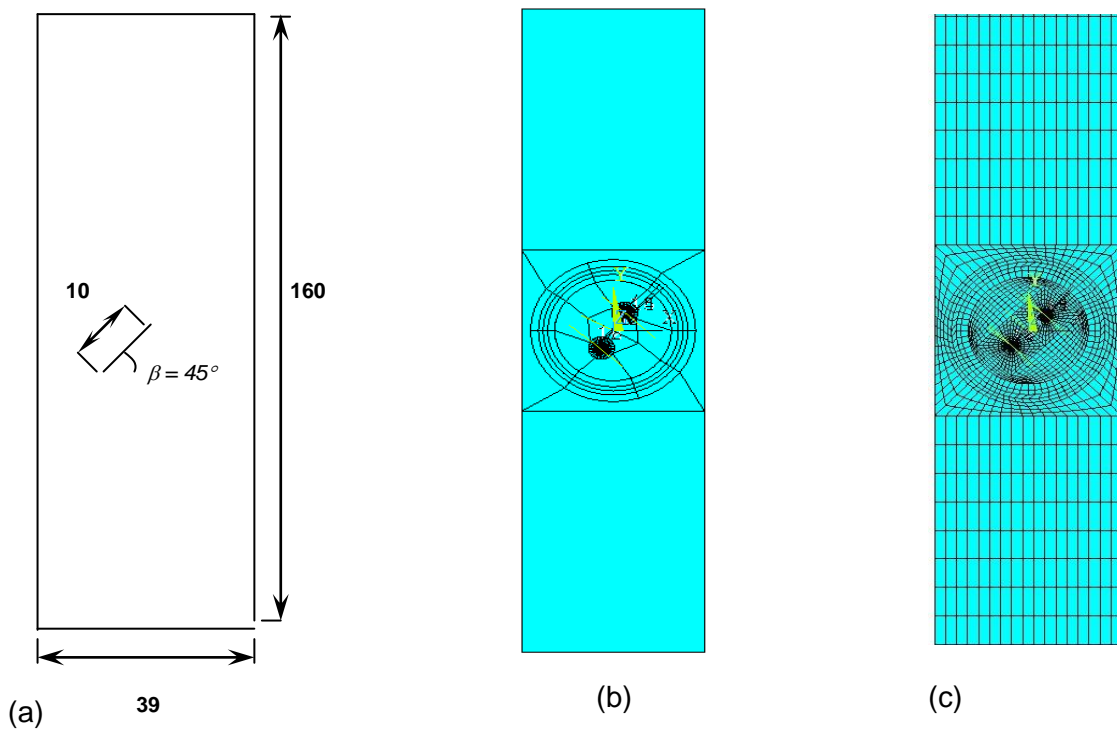


**Fig 2.5:** The panel area panel geometry (a) before meshing and (c) after meshing for a circular patch

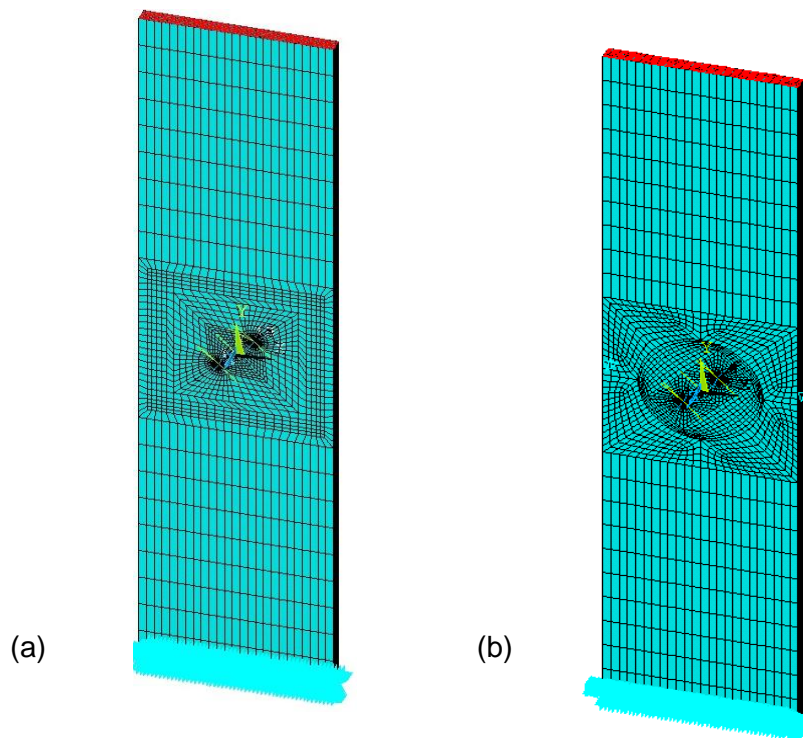


**Fig 2.6:** The panel volume after meshing for (a) rectangular patch (b) circular patch

## 2.4.2 Modeling of Patch and Adhesive

The mesh pattern at the interface areas must be same as coupling is being used for mimicking the adhesive behavior. In case of MPC coupling, the mesh pattern of the adjacent surfaces need not be the same. The 2D mesh pattern similar to the panel is created for the required patch geometry. The only difference being that the crack is absent. Then, the area is extruded to create the volume and the area mesh is swept through this volume similar to that of the panel. The thickness of adhesive is 0.1 mm (extruded from  $z = 0$  to  $z = 0.1$  mm) and it has got two elements across its thickness. The thickness of patch is 1.5 mm (extruded from  $z = 0$  to  $z = 1.5$  mm) and it has four elements through its thickness. The meshed patch and adhesive is shown in Figure 2.7. For coupling of the surfaces, the nodes on the adhesive along the adjoining surfaces should be grouped as a component and similarly for the patch side too. For single sided repair, the patch needs to be shifted by 0.1 mm in positive  $z$  direction. For double sided repair the adhesive on the other side has to be shifted by -3.275 mm and the patch needs to be shifted by -4.775 mm. The adhesive and patch model is created as separate database files.

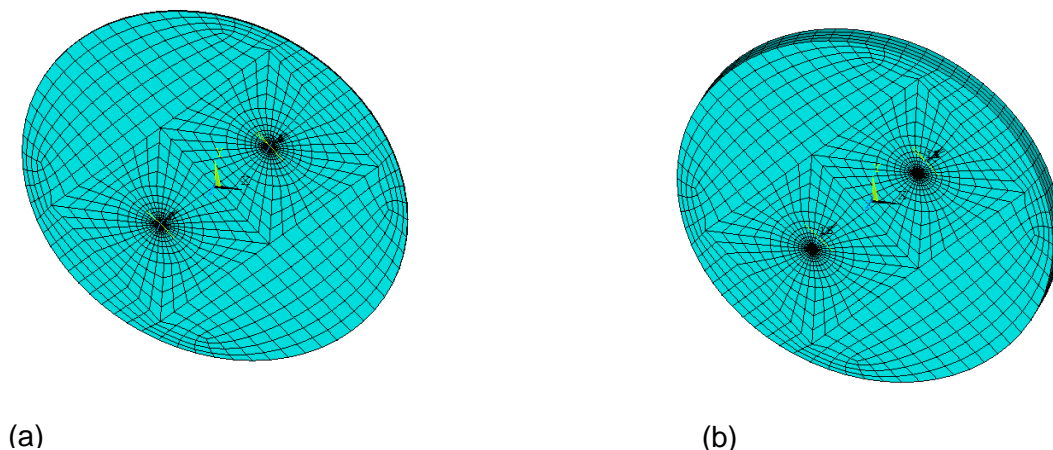


**Fig 2.7:** The 3D mesh for (a) circular adhesive (b) circular patch

### 2.4.3 Assembly of composite repair model

After saving the panel, adhesive and patch, they are in .db format. In order to bring the adhesive and patch into the panel file, they must be saved in .cdb format. These .cdb format files contain only nodes and elements. After the adhesive and patch file is brought into the panel database, the nodes at the interface surfaces should be coupled in any of the methods stated above. The material property is assigned by selecting the components separately and assigning them the material properties. The patch being an orthotropic material will require an element coordinate system to be defined locally which can give directional material properties. The material properties of the assembly are as shown in the table 2.1. In case of defining unbalanced laminated, elements belonging to each patch layer are picked and then assigned different element coordinate system. In case of transversely graded material, the patch properties are defined as isotropic and each layer is given the material properties separately as per variation. After this, the model is solved with appropriate boundary conditions.

### 2.5 Validation of Results

Stress intensity factor values were validated for the panel model having straight center crack against the analytical equation. The analytical equation for SIF for a centre cracked semi-infinite plate with finite width is given as [28].

$$K_I = \sigma \sqrt{(\pi a)} f(\alpha) \quad (2.3.1)$$

where,

$2a$  is the crack length

$W$  is width of the panel

$$\alpha = \frac{a}{W}$$

$$f(\alpha) = 1 + 0.128\alpha - 0.288\alpha^2 + 1.523\alpha^3 \quad (2.3.2)$$

From this the value of SIF in mode-I for a 0 degree crack is found to be 487.02 MPa√mm

The value of  $K_I$  obtained from FE analysis in this work is 503.61 MPa√mm which is in close agreement with the analytical value (See table 2.2)

For the 30, 45 and 60 degree cracks being mixed-mode cracks, mode II also exists. The components of stress in the directions along the crack and perpendicular to it are

$$\sigma_n = \sigma \cos^2 \beta \text{ which is the component of applied stress perpendicular to crack front}$$

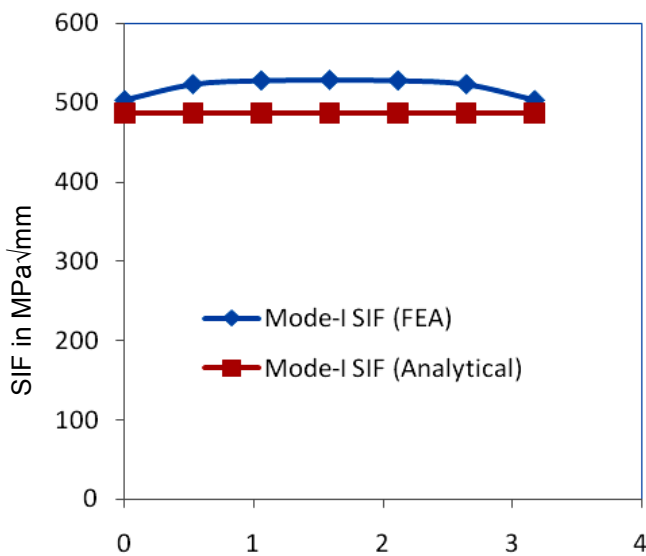
$$\sigma_t = \sigma \cos \beta \sin \beta \text{ which is the component of stress along the crack front}$$

Using these values the SIF values in mode-I and mode-II is solved analytically.

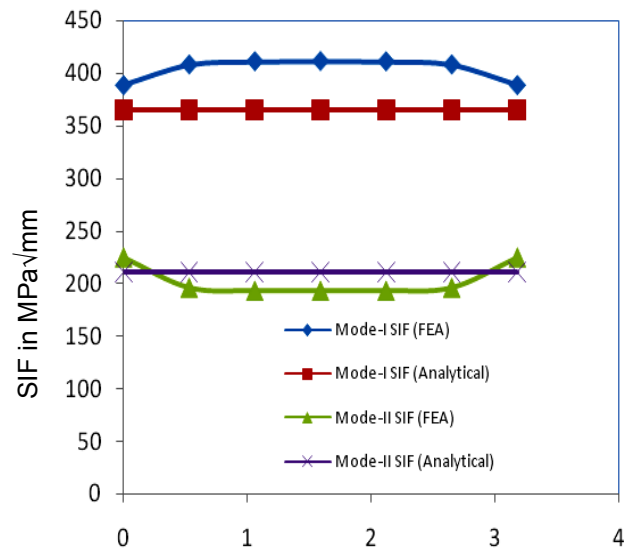
**Table 2.2** Comparison of SIF at the panel surface solved by analytical and numerical methods (All units in MPa√mm)

Crack Inclination Angle	$K_I$ (Analytical)	$K_I$ (FEA)	$K_{II}$ (Analytical)	$K_{II}$ (FEA)	$K_I$ % error	$K_{II}$ % error
0	487.02	503.61	0	0	3.40	
30	365.26	388.32	210.88	224.75	6.31	6.57
45	243.51	265.13	243.51	267.54	8.88	9.86
60	121.75	133.72	210.88	238.79	9.82	13.2

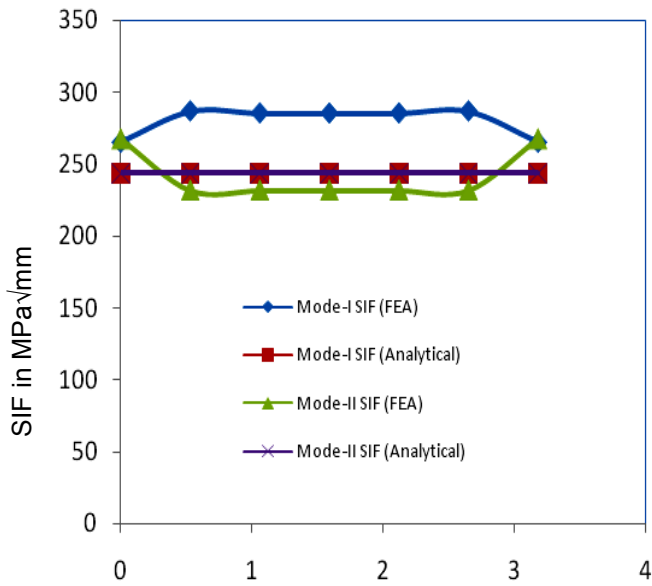
From the above table, we can see that there is a good match between analytical and numerically solved models with error being less than 10%. The error is because in the analytical expression we consider the semi-infinite plate where as in FEA analysis a finite plate is considered.



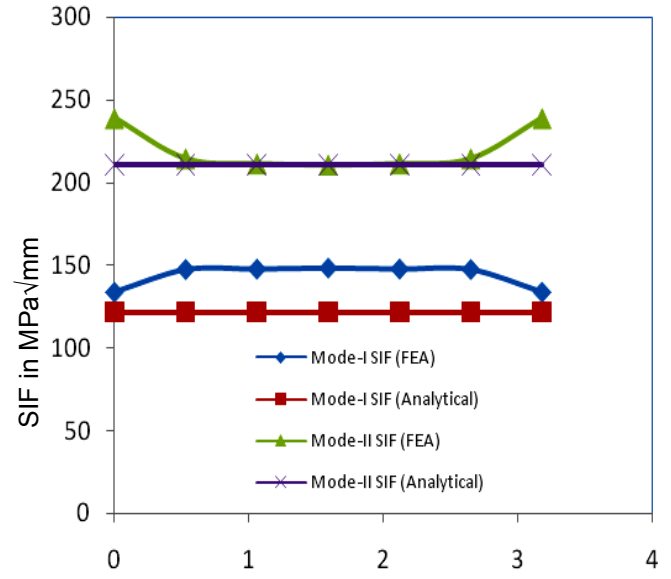
(a) Thickness through the panel in mm



(b) Thickness through the panel in mm



(c) Thickness through the panel in mm



(d) Thickness through the panel in mm

**Fig 2.8:** Variation of SIF through the thickness for an un-patched crack inclination angle of (a) 0 degree (b) 30 degree (c) 45 degree (d) 60 degree

To further re-verify the meshing requirements, the variation of  $J$ -integral value for different ply orientations is carried out for 1.5 mm thick patch. The results are compared with the results obtained by Toudeshky [23]. From Figure 2.9 one can notice that the variation of  $J_{\text{mid-plane}}/J_{\text{un-repaired}}$  is found to be in agreement with the reference [23] thus confirming the correctness of our procedure. Also the mesh size considered is sufficient enough to carry out the analysis.

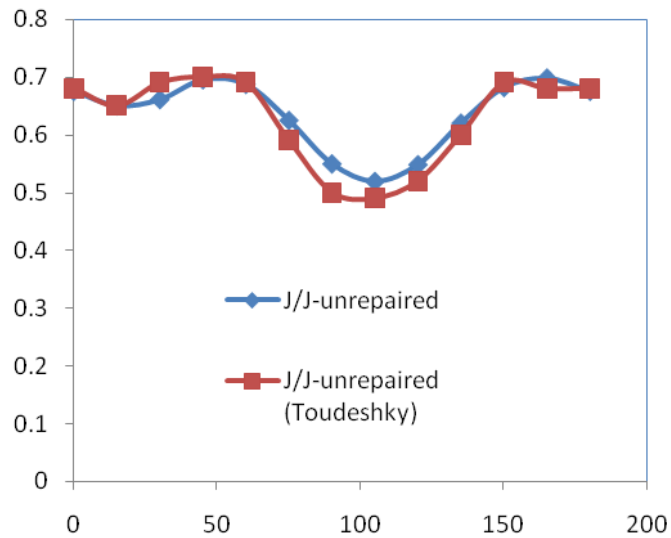


**Fig 2.9:** Variation  $J/J_{\text{unrepaired}}$  for different patch orientations for a 1.5 mm thick patch given by reference [23] and present work

## 2.6 Closure

The results in this work are in agreement with the work carried by Toudeshky and also with the analytical expressions. Therefore the above described model is suitable for carrying out further numerical analysis. The finite element mesh chosen is able to predict the fracture parameter with greater accuracy. It also gives us the confidence in applying the model for further repair analysis.



# Chapter 3

## Modeling and analysis of double sided composite repair

### 3.1 Introduction

In order to extend the life of an aircraft, many factors need to be considered. One such parameter is the growth of cracks. Repair of the cracks is feasible only if the number of cracks are minimum and the size of the crack is small compared to the panel. Adhesively bonded repairs have now replaced the riveted patches for the numerous advantages it possesses over mechanical fasteners. The adhesively bonded repairs are carried out in two ways – single and double sided repair. In double sided repair, the both faces of the crack front are patched and in single sided repair only once side of the crack is patched. For this to be possible, both faces of the panel must be available for patching. But in very few instances, this is possible.

Double sided repair is more preferred to single sided repair for numerous reasons. It offers resistance to crack opening on both faces increasing the area over which resistance is provided, thereby performing better than single sided patch. Also due the symmetry of its geometry, there is no shift of neutral axis in patched panel (I.e. same as panels neutral axis) which does not create any out of plane bending. Even if the thermal expansion coefficients for patch and panel are different, any bending of the panel will not take place. Most works in literature concentrate on the single sided patching rather than the double sided patching. This is because in most practical cases, only one side of the panel is available for repair such as aircraft wings.

In this chapter, we study the effect of patch applied on panels having mixed mode cracks of different angles. Also the impact of different patch geometries for a given

area is studied for the 45 degree crack. All the fibres of the patch are aligned along the loading direction. This kind of alignment would maximize the reinforcement. Since bending is absent in double sided patching, the analysis is straight forward.

The FE modelling is done according to the procedure mentioned in chapter 2. The number of equations is in 900,000 range and it takes much more time than solving the single sided repair. The schematic of the repair is given in the Figure 3.1. Since bending of the panel is absent in double sided repair, we only four elements through panel thickness instead of six.

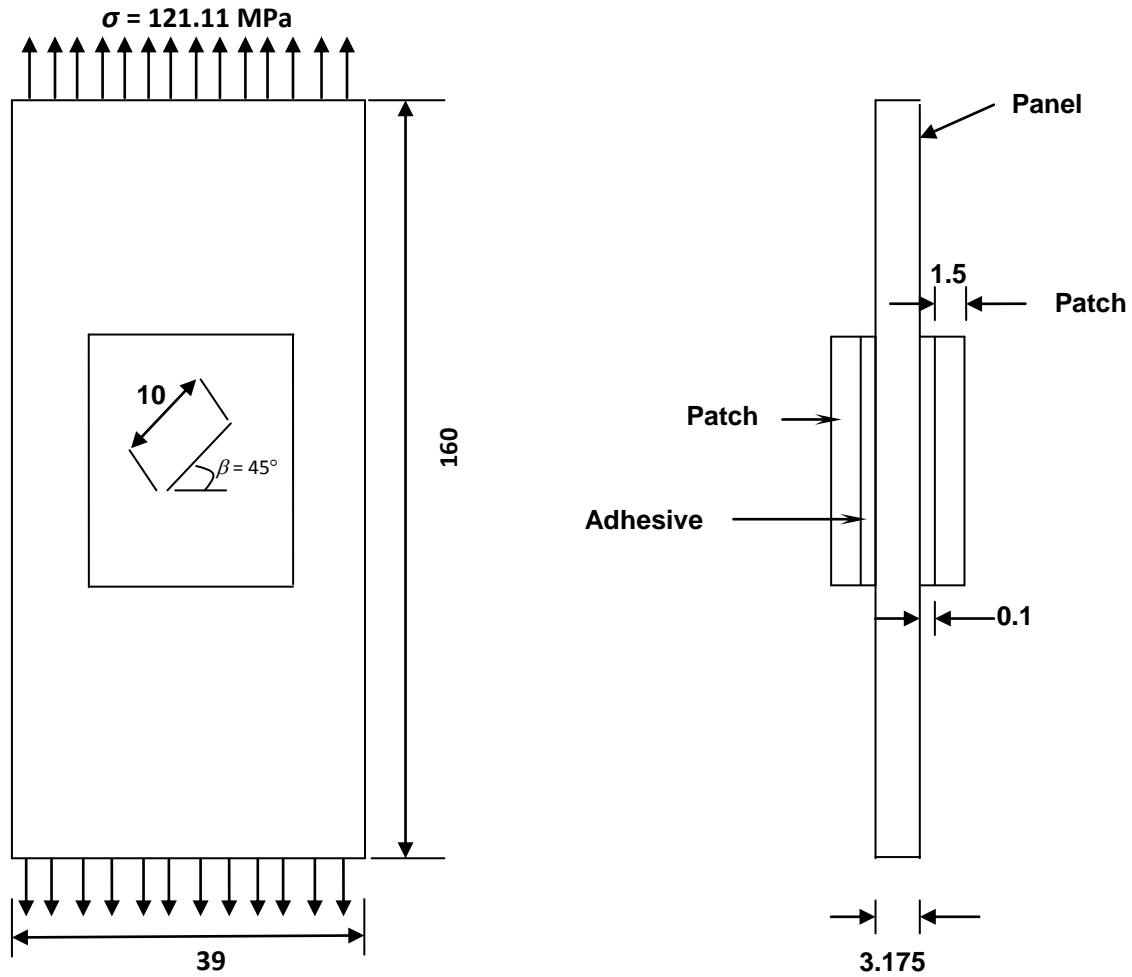


**Figure 3.1:** Geometry of panel with crack (all units in mm)

### **3.2 Patch Material**

The properties of the repair elements is shown in Table 2.1. The panel is made of Aluminum alloy 2024-T3 which is widely used in aircraft structures. The adhesive used is FM-77. The patch material is made of boron epoxy composite laminate. The high directional stiffness restricts the crack opening on the panel. Most repair applications use unidirectional laminates which gives reinforcement in the loading direction. In case of bi-axial loading, the unbalanced laminates are used. The only disadvantage is the mismatch of the thermal expansion coefficients which can cause additional bending when subjected to a range of temperatures. Metallic patches being isotropic can offer resistance to multi-axial loading, but most repairs are subjected to uniaxial load where composite laminate is a better option.

### **3.3 Modeling**

The modeling is done as mentioned in the previous chapter. The analysis has been carried out for crack inclination angles of 30°, 45° and 60° in the panel. The 30° degree is a case where mode-I is more dominant than mode II and 60° is a case where mode-II is more dominant than mode-I. In case of 45° crack SIF in both mode I and mode II are of equal value. The different patch shapes seen were analyzed are ellipse, circle, octagon and rectangle. All the patches are centered on the panel above the crack. The ellipse was chosen such that the ratio of minor axis to major axis is 0.8 and the semi major axis length varies from 12.5 to 17.68 mm. The radii of circle varied from 12.5 to 17.68 mm. The height of the rectangle is 25 mm and its length is varied from 28 mm to 35.36 mm.

### 3.4 Results and Discussion

#### 3.4.1 Elliptical patch shape

The dimensions of the ellipse chosen are such that the ratio of minor axis to major axis is 0.8. The major axis is perpendicular to the loading direction. The variation of SIF through the thickness show similar trends for both modes of fracture. The elliptical patch is centred on the panel to be repaired. Firstly elliptical patch is considered. Figure 3.2 shows the SIF variation through the panel thickness having an inclined crack at 30 degrees. Looking at the figure, one can ascertain that ellipse with larger major axis has largely reduced the SIF. Figure 3.3 shows the SIF variation for the repaired panel having crack inclination of 45 degrees. Trend observed is the patch with larger major axis has performed better in terms of SIF reduction. This is because more area is available for load transfer and hence reduction in SIF. Figure 3.4 shows the SIF variation through the panel thickness having an inclined crack at 60 degrees. Here too, the same trend is observed and the patch with larger major axis has performed better in terms of SIF reduction

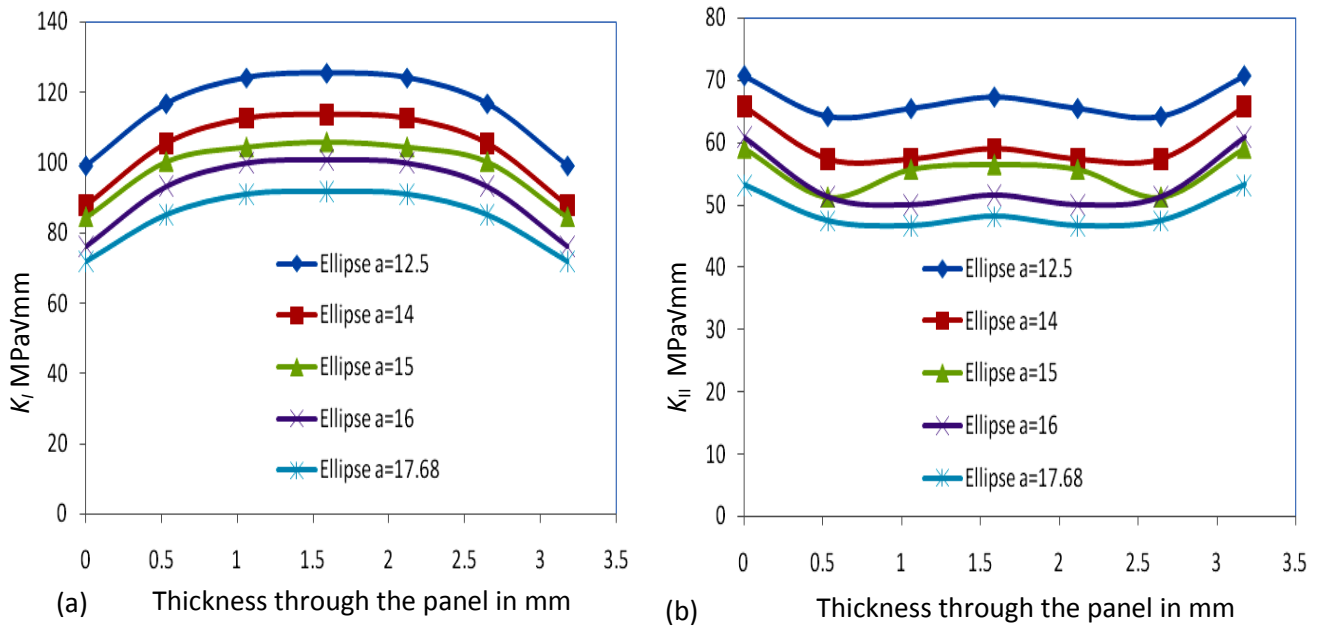
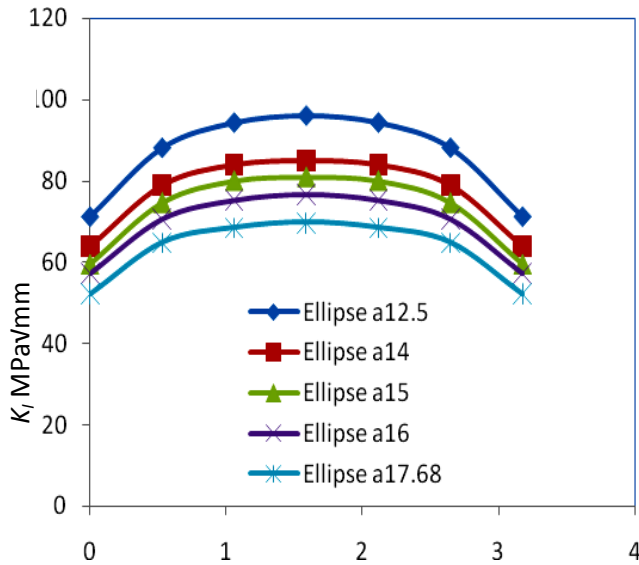
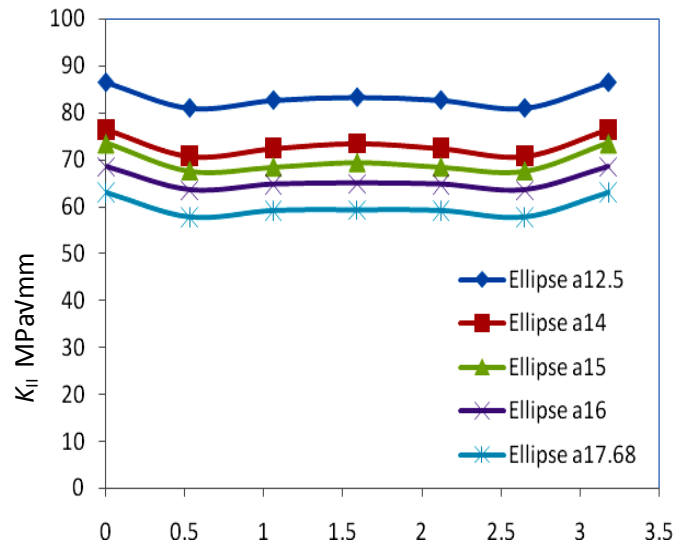


**Fig 3.2:** Variation of SIF through the thickness for double sided an elliptical patch for 30 degree crack (a)  $K_I$  (b)  $K_{II}$

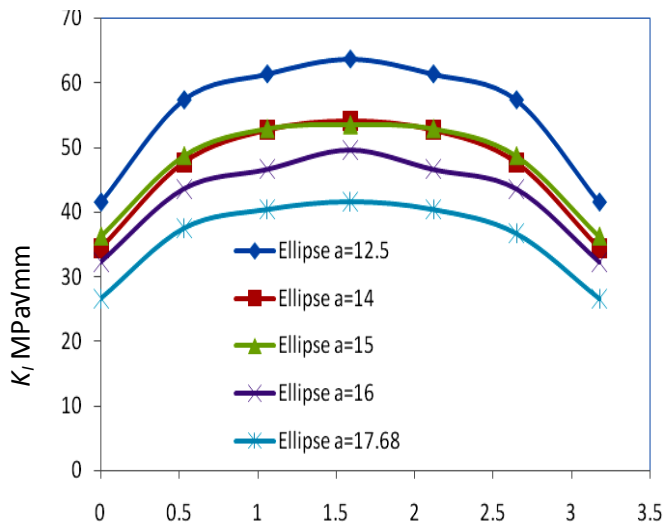


(a) Thickness through the panel in mm

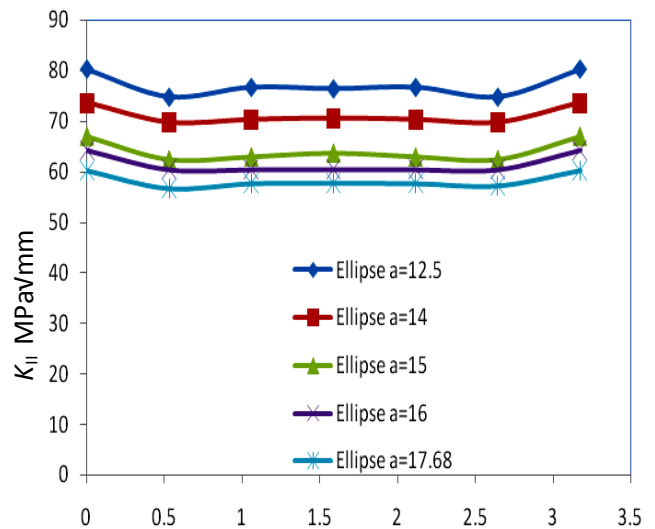


(b) Thickness through the panel in mm

**Fig 3.3:** Variation of SIF through the thickness for double sided an elliptical patch for 45 degree crack (a)  $K_I$  (b)  $K_{II}$



(a) Thickness through the panel in mm



(b) Thickness through the panel in mm

**Fig 3.4:** Variation of SIF through the thickness for double sided an elliptical patch for 60 degree crack (a)  $K_I$  (b)  $K_{II}$

To summarize from the Figures 3.2, 3.3 and 3.4 it is evident that for different modes of fracture, the ellipse with major axis 17.68 mm has performed better. For the 30 degree repaired crack, the  $K_I$  is much higher than the 45 and 60 degree cracks. For the 45 and 60 degree crack,  $K_{II}$  is the maximum. Comparing their performance, one can easily say that in case of elliptical patches, it is better to use the one with the maximum major axis.

### **3.4.2 Circular Patch shapes**

The different radius of circle chosen is same as the semi-major axis of the ellipse. Trends observed are similar to the ellipse. The circular patch is symmetric about the crack for any crack inclination angle. Firstly circular patch is considered. Figure 3.5 shows the SIF variation through the panel thickness having an inclined crack at 30 degrees. Looking at the figure, one can ascertain that circle with larger radius has largely reduced the SIF. Figure 3.6 shows the SIF variation for the repaired panel having crack inclination of 45 degrees. Trend observed is the patch with larger radius has performed better in terms of SIF reduction. This is because more area is available for load transfer and hence reduction in SIF. Figure 3.7 shows the SIF variation through the panel thickness having an inclined crack at 60 degrees. Here too, the same trend is observed and the patch with larger radius has performed better in terms of SIF reduction

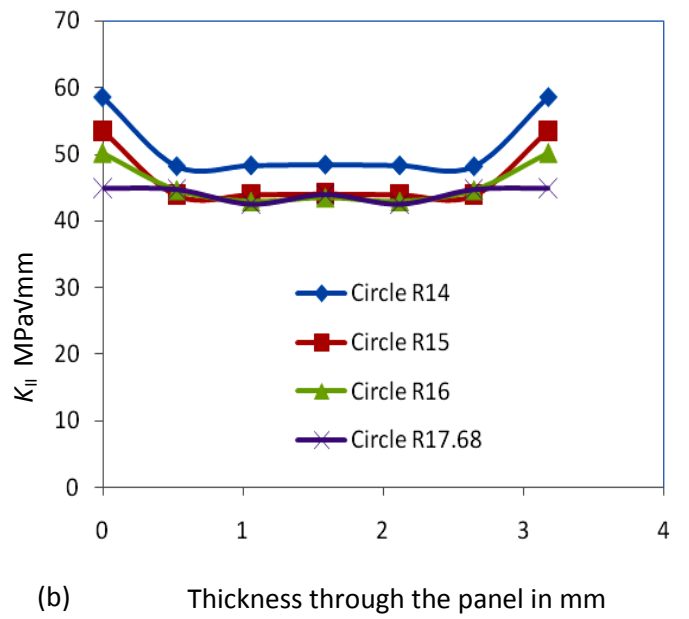
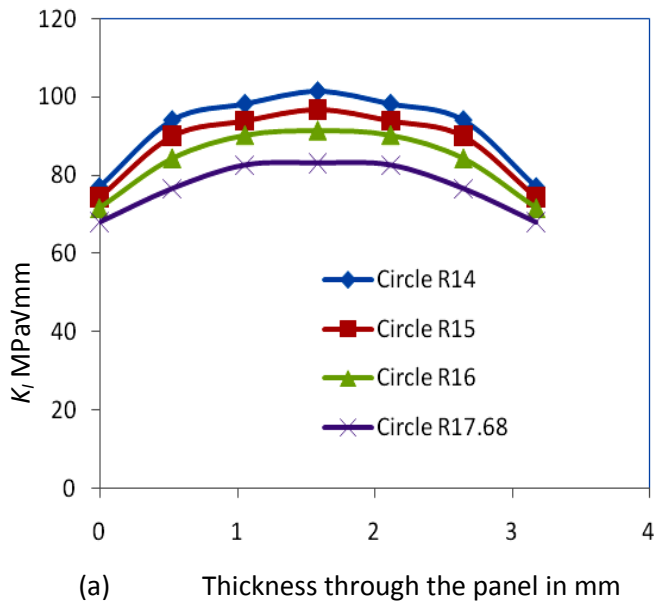


**Fig 3.5:** Variation of SIF through the thickness for double sided an circular patch for 30 degree crack (a)  $K_I$  (b)  $K_{II}$

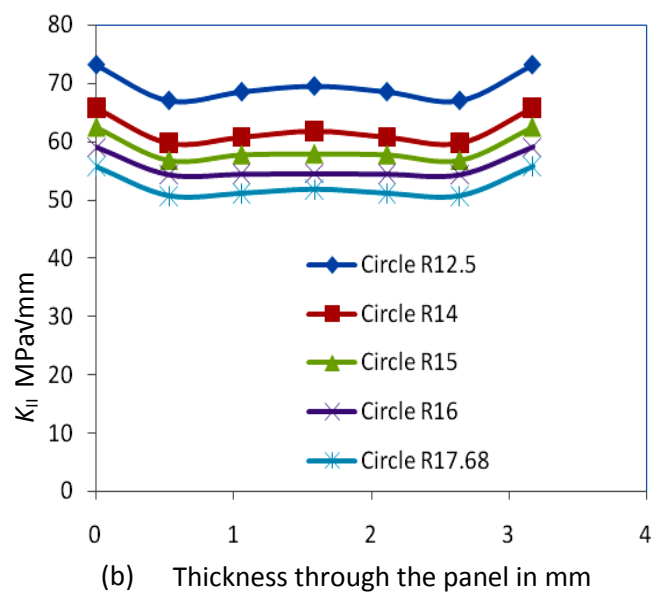
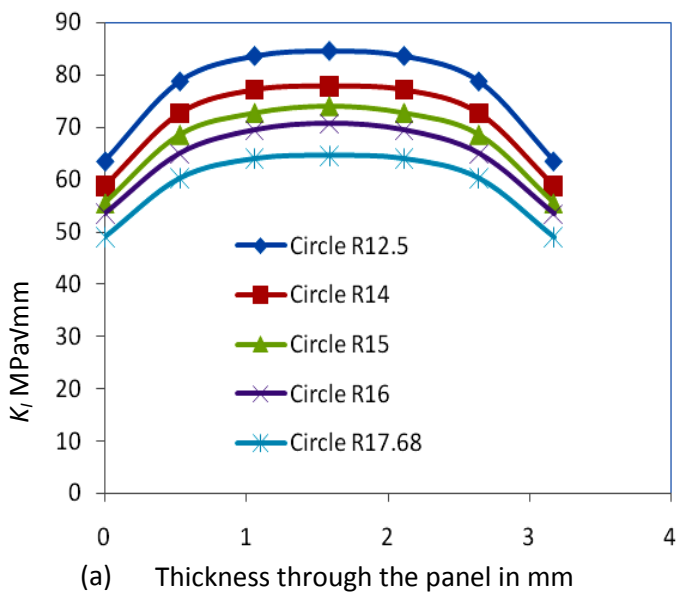


**Fig 3.6:** Variation of SIF through the thickness for double sided an circular patch for 45 degree crack (a)  $K_I$  (b)  $K_{II}$

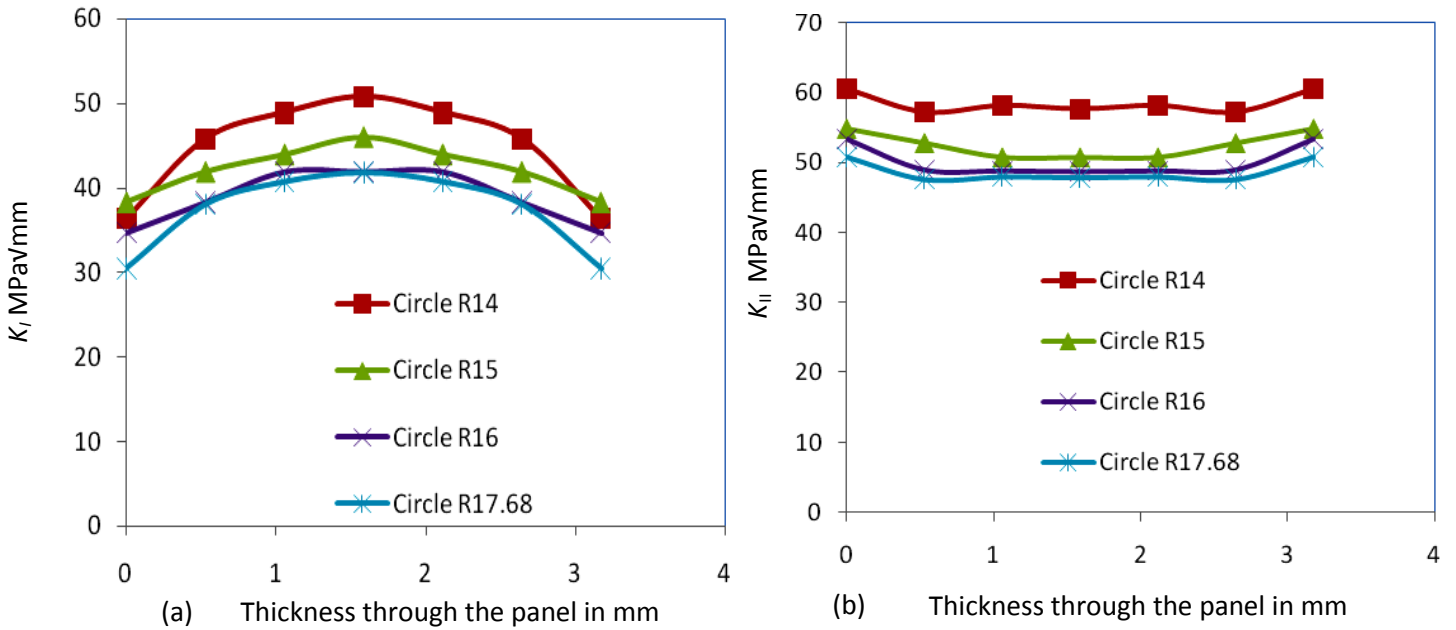


**Fig 3.7:** Variation of SIF through the thickness for double sided an circular patch for 60 degree crack (a)  $K_I$  (b)  $K_{II}$

From figures 3.5, 3.6 and 3.7 one can see that the circle for the radius 17.68 is best in handling the SIF in both modes, hence we can conclude that the larger the area of patch, the better. Also as the radius increases, the decrease in SIF is smaller compared to the previous case. The mode I SIF is maximum for the 30 degree crack and least for 60 degree crack.

### 3.4.3 Rectangular Patch Shape

The rectangular patch chosen is such that the width is varied keeping the height constant. One of the dimensions of the rectangle is same as the diameter of circle considered previously. The height of the rectangle chosen is 25 mm and the width is varied from 25 mm to 35.36 mm. Firstly rectangular patch is considered. Figure 3.8 shows the SIF variation through the panel thickness having an inclined crack at 30 degrees. Looking at the figure, one can ascertain that rectangle with larger width has largely reduced the SIF. Figure 3.9 shows the SIF variation for the repaired panel having crack inclination of 45 degrees. Here too, the same trend is observed and the patch with larger width has performed better in terms of SIF reduction. This is because more area is available for load transfer and hence reduction in SIF. Figure 3.10 shows the SIF variation through the panel thickness having an inclined crack at 60 degrees.



Here too, the same trend is observed and the patch with width has performed better in terms of SIF reduction

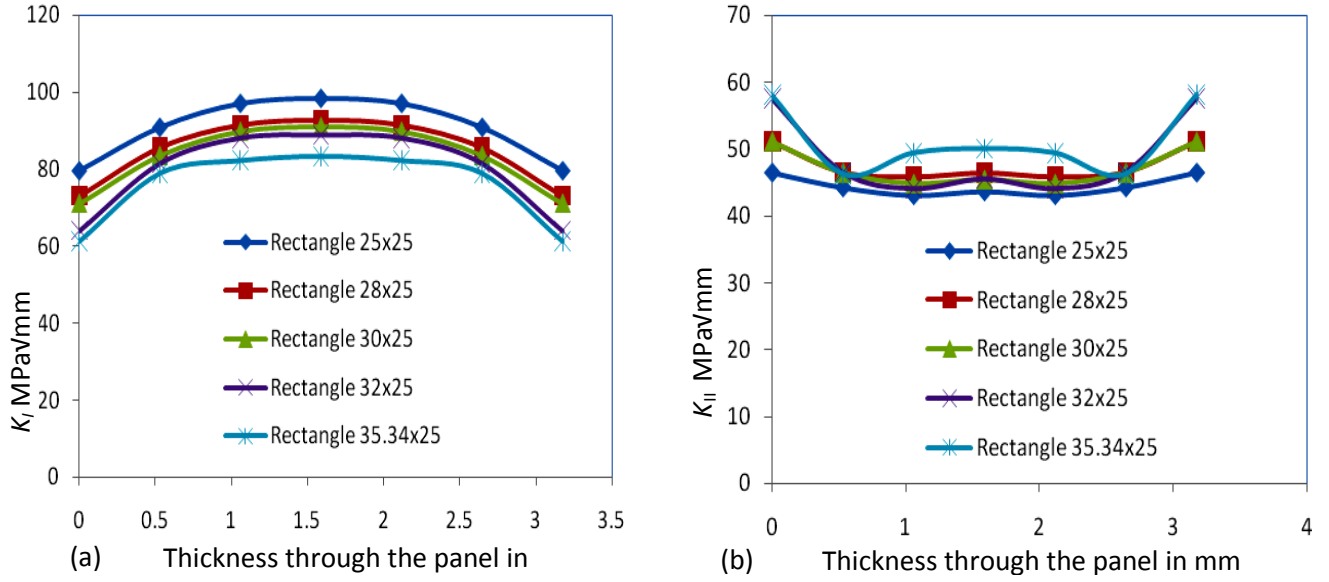


**Fig 3.8:** Variation of SIF through the thickness for double sided an rectangular patch for 30 degree crack (a)  $K_I$  (b)  $K_{II}$

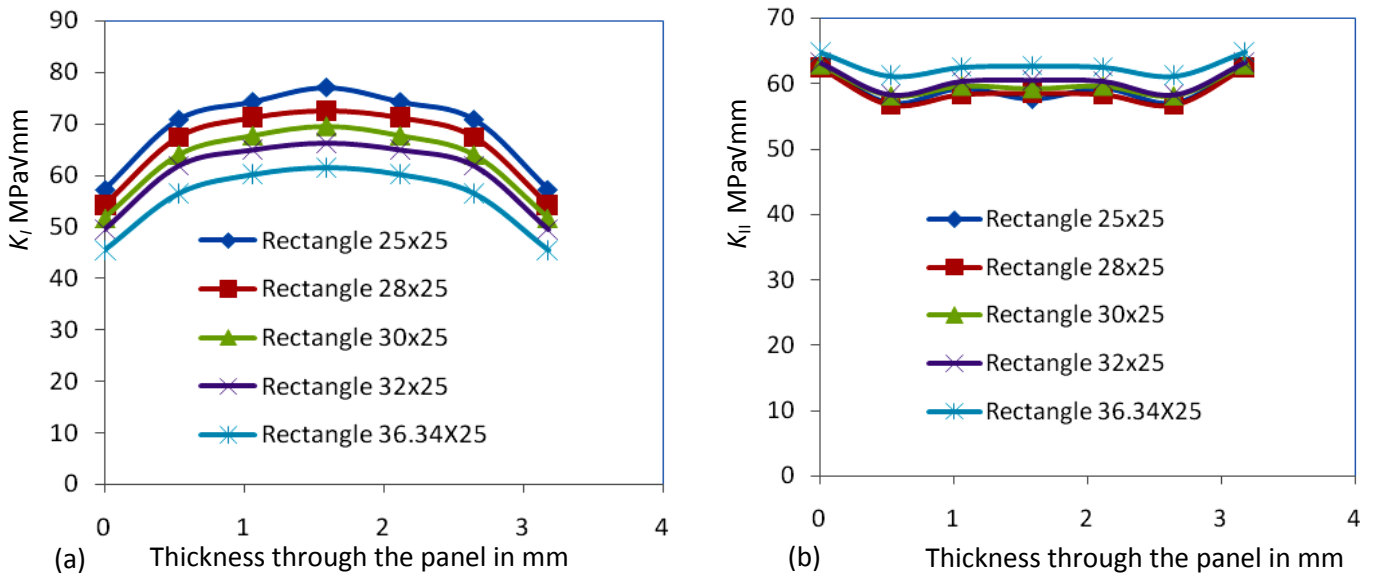


**Fig 3.9:** Variation of SIF through the thickness for double sided rectangular patch for 45 degree crack (a)  $K_I$  (b)  $K_{II}$

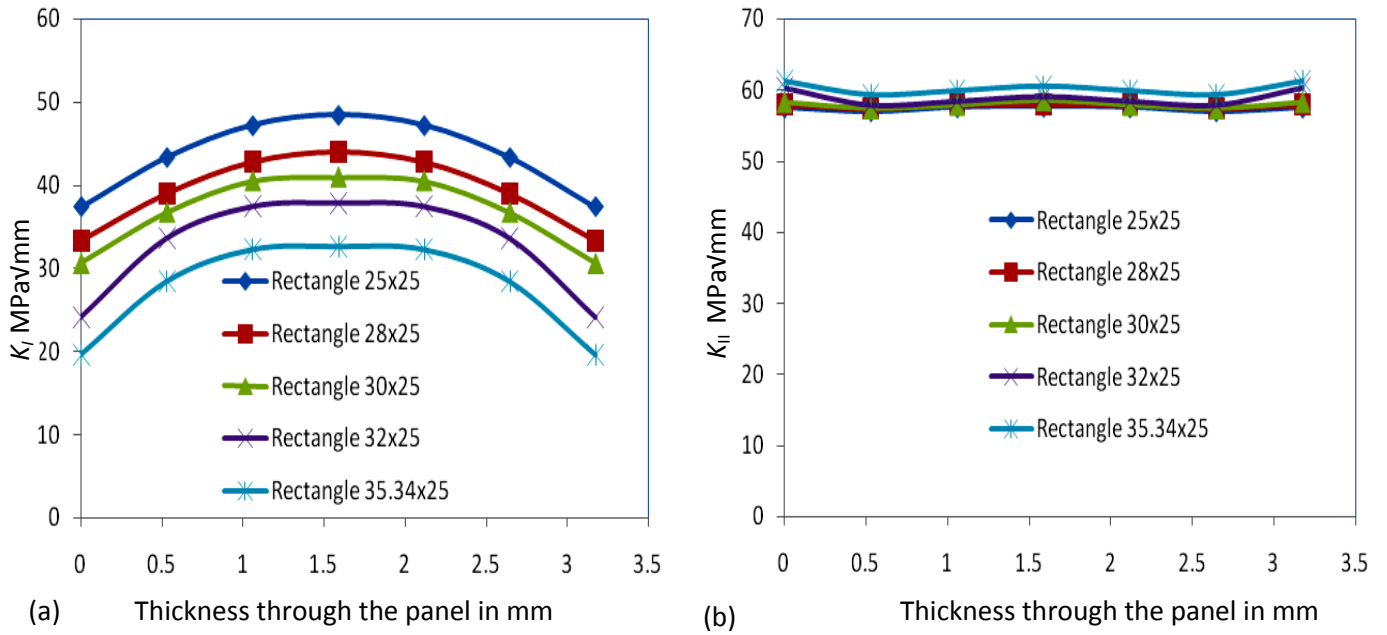


**Fig 3.10:** Variation of SIF through the thickness for double sided rectangular patch for 60 degree crack (a)  $K_I$  (b)  $K_{II}$

The graph in figures 3.8, 3.9 and 3.10 are for constant height and is obtained by varying the widths.  $K_I$  keeps decreasing with increasing width.  $K_{II}$  is lowest for the 30 degree patch and is almost same for 45 and 60 degree cracks.  $K_I$  is the maximum in 30 degree crack and minimum for 60 degree crack. It is seen that graphs of  $K_{II}$  in repaired model are very close indication that the patch width has little effect in mode II fracture.

**Table3.1.** Different patch shapes and their areas

S.No	Shape	Semi-Major axis ( $a$ ) in mm	Semi-Minor axis ( $b$ ) in mm	Area in mm <sup>2</sup>
1	Ellipse	12.5	10	392.5
		14	11.2	492.352
		15	12	565.2
		16	12.8	643.072
		17.68	14.144	785.207
2	Circle		Radius	Area
			12.5	490.625
			14	615.44
			15	706.5
			16	803.84
	17.68	981.5087		
3	Rectangle	Width	Height	Area
		25	25	625
		28	25	700
		30	25	750
		32	25	800
	35.36	25	884	
4	Regular Octagon		Side	Area
			15.79	706
			16.81	800
		18.62	981	

### 3.5 Area Normalization

The following analysis is done for a given area of a patch for which the shapes are varied. The analysis is done for a panel having a 45 degree crack and the patch thickness is 1.5 mm. The different patch areas considered are 981, 803 and 706 mm<sup>2</sup> which correspond to the area of circle with radius 17.68, 16 and 15 mm respectively. The different shapes chosen in the study are rectangle in which width is more than height, rectangle in which height is more than width, square, circular and elliptical. Ellipse (b>a) is the ellipse in which the minor axis is greater than the major axis. From the Figures 3.11, 3.12 and 3.13 it can be seen that as the length of rectangle increases, the  $K_I$  decreases. Similarly when the height of the rectangle increases,  $K_{II}$  decreases. Also noticeable is that for the rectangle with maximum width,  $K_I$  is lowest but  $K_{II}$  is highest. Similarly for the rectangle with maximum height, the  $K_{II}$  is lowest but  $K_I$  is highest. Overall as the larger the area of patch, the lower is the SIF. Since we need to reduce both  $K_I$  and  $K_{II}$  effectively, we can conclude that the circle is the best shape for the given area as it covers an equal extent over the crack.

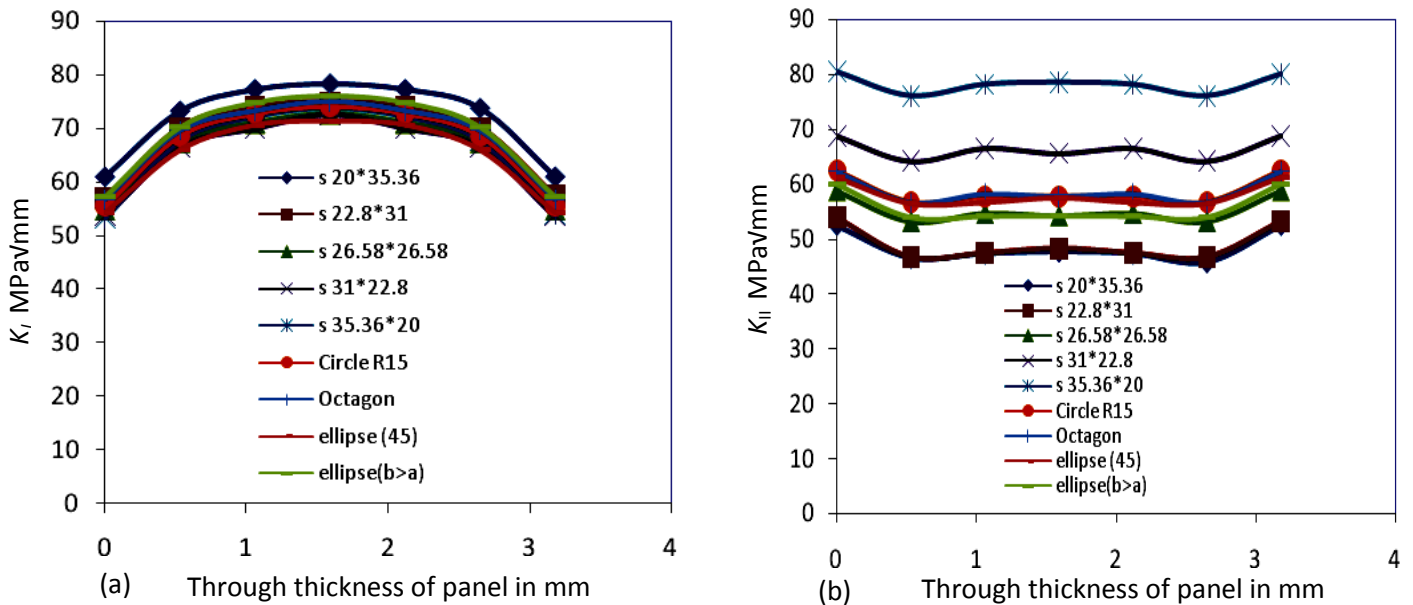


**Fig3.11:** Variation of SIF through the thickness for double sided patch of area 706mm<sup>2</sup> (a)  $K_I$  (b)  $K_{II}$

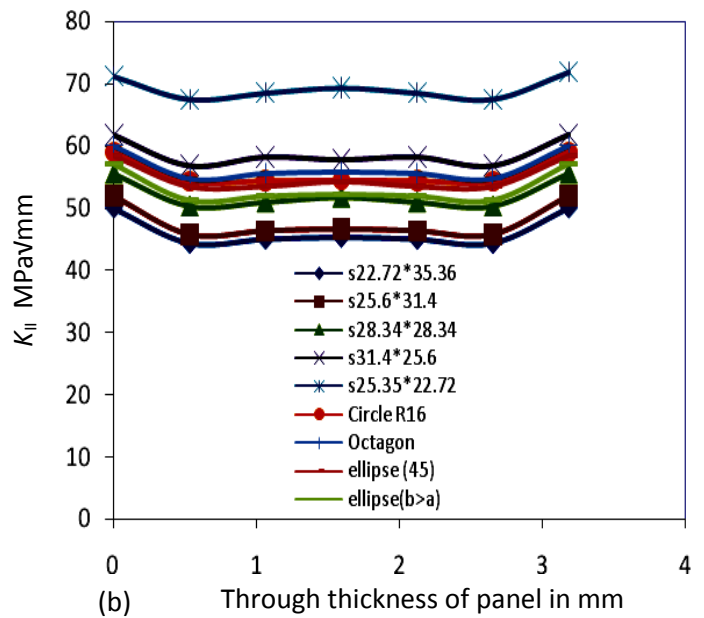
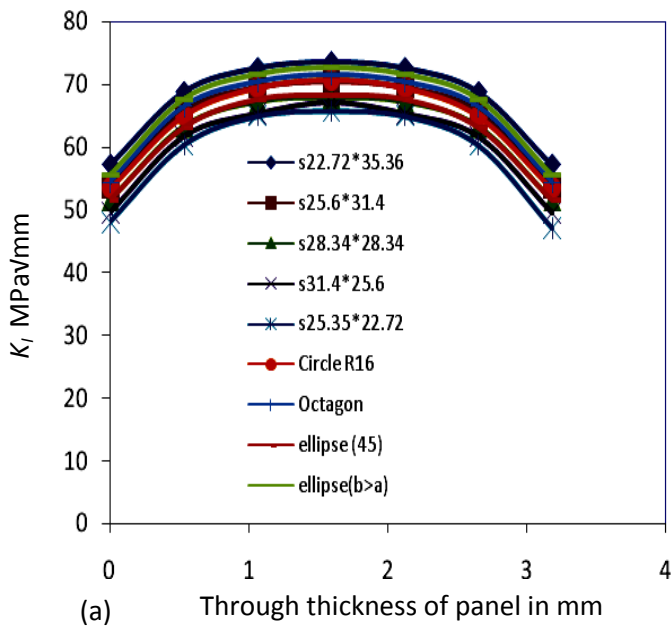


**Fig.3.12:** . Variation of SIF through the thickness for double sided patch of area 800mm<sup>2</sup> (a)  $K_I$  (b)  $K_{II}$

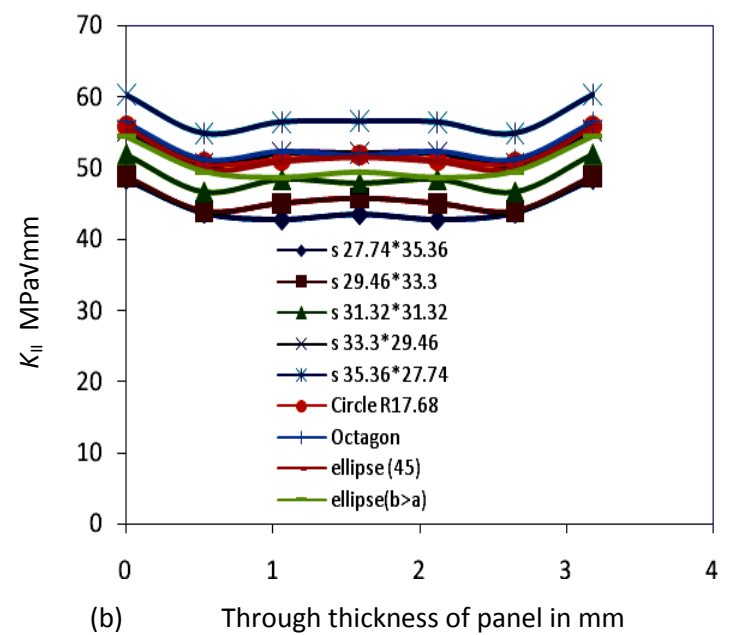
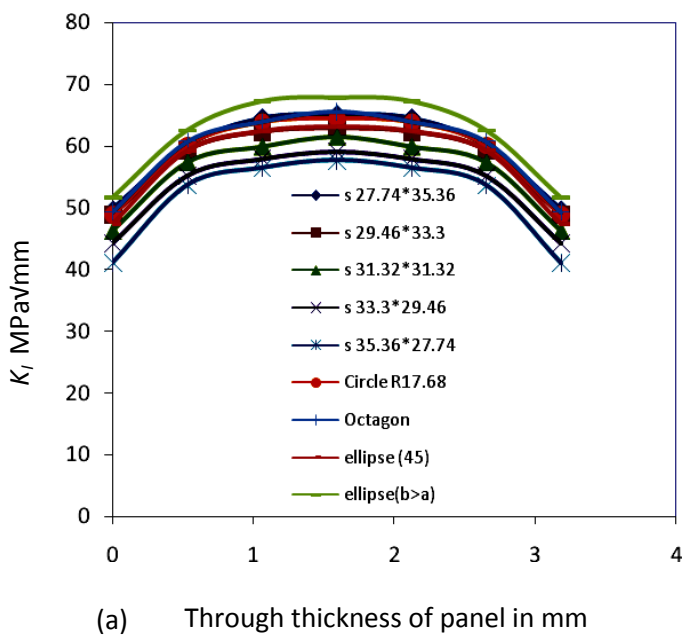


**Fig.3.13:** Variation of SIF through the thickness for double sided patch of area 981mm<sup>2</sup> (a)  $K_I$  (b)  $K_{II}$

### 3.6 Closure

Among the different crack inclination angles, the 30 degree crack has the maximum  $K_{II}$ . The 60 degree crack gives lowest values in both modes. Also as the area of the patch over the crack increases, the SIF reduces due to the higher stiffness over the crack area locally. When the length of the rectangle is increased,  $K_I$  reduces and as the height of the rectangle increases,  $K_{II}$  decreases. Hence a trade off must be considered. The circular patch which has equal extension in both directions is the considered to be an optimum patch shape. Since the component of load along the crack is highest in case of 60 degree crack, it is expected that the 60 degree crack has the highest  $K_{II}$  for the given load. However the  $K_{II}$  values for the 60 degree crack is similar to the 45 degree crack because the crack opening in case of 60 degree crack is the least.

# Chapter 4

## Modeling and analysis of single sided composite repair

### 4.1 Introduction

Most of the adhesively bonded composite patch repair is performed on aircraft structure. In single sided repair, only one face of the panel is repaired such as aircraft wings. Though the double sided repair is a better option compared to the single sided repair, in most practical cases only one face of the panel is available for repair. Modelling of unsymmetrical repair is very challenging because of the presence of out of plane bending for tensile loads also. Due to the repair configuration being asymmetric, there is a shift of the neutral axis away from the panel increasing the distance between the up-repaired surface and the neutral axis. Since the bending stresses are proportional to distance from neutral axis, there is more bending stresses present at the unrepaired surface which causes bending. The mechanics and behaviour of single sided patch repair is completely different from double sided patch. Though 3 elements are sufficient to be taken along the panel, here we consider six in order to capture the bending effect; otherwise the panel will be too stiff to bend.

The analysis is done a mixed mode cracks of different crack inclination angles (30,45 and 60 degree). The panel geometry is same as the one considered for the double sided repair. The modelling is done as stated in chapter 2. The number of equations is in the 500,000 range and takes much less time than a double sided repair. The schematic of single sided repair is shown in Figure 4.1.

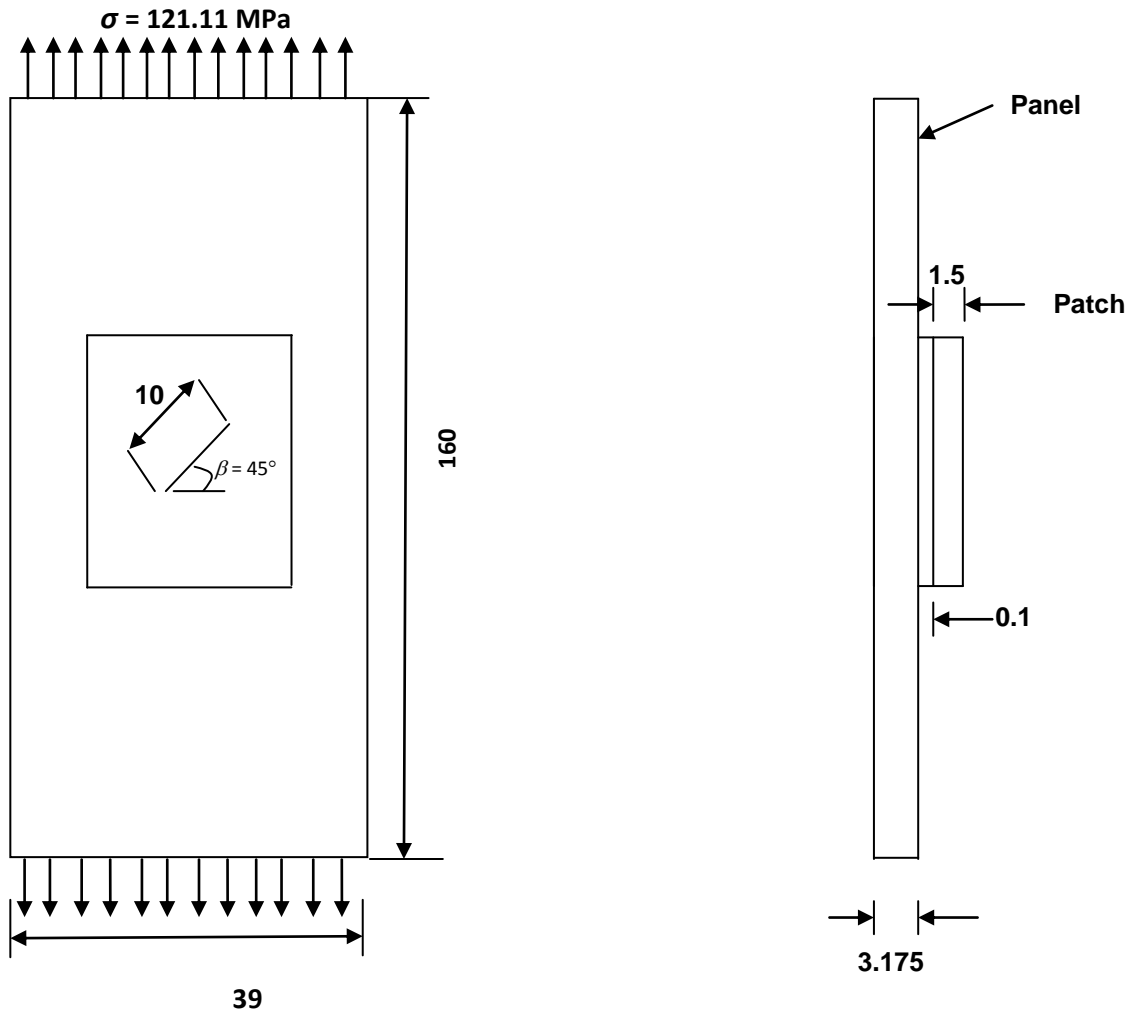


**Figure 4.1:** Geometry of panel with crack for single sided repair(all units in mm)

## 4.2 Patch materials

The panel material is made of aluminium alloy. The selection of the patch material is the most important part of the single sided repair. In this work, boron-epoxy laminates is used as reinforcement. The patch is 1.5 mm thick and there are four layers of the laminates each layer thickness being 0.375 mm. To start with, unidirectional laminate having fibres aligned along the loading direction is chosen as patch material. Later



analysis is carried out for the panel having reinforcement made of un-balanced laminate and transversely graded material. The properties of the materials are given in table 3.1.

### **4.3 Single side patch for different crack inclination angles using unidirectional laminates**

Firstly the analysis of the single sided repair is done using unidirectional laminates aligned along loading direction. The patch geometry is a rectangle with varying heights. The thickness of the patch is 1.5 mm. From the Figures 4.2, 4.3 and 4.4 it is seen that the SIF values for a single sided repair is almost independent of the patch geometry. However for different crack inclination angles, the SIF values are different. It is also seen that the SIF is maximum at the un-repaired side. From Figure 4.2, it is seen that  $K_I$  is much higher than  $K_{II}$  for the 30 degree crack. From Figures 4.3 and 4.4, it is seen that  $K_{II}$  for the 60 degree crack is lower than the 45 degree crack even though the stresses causing mode-II fracture in 60 degree crack is higher than that of 45 degree crack. Hence we can say that for a given crack inclination angle, SIF values are independent of patch geometry. Also the value of mode-I SIF at the un-patched side is much higher than the unrepaired side. This is because of the shift of neutral axis towards the patch leading to increased bending stress at the un-patched side. Since the patch geometry has little effect on the fracture parameters, the patch has to be designed such that it counters the bending. The unbalanced laminates have this feature to produce counter bending effect.

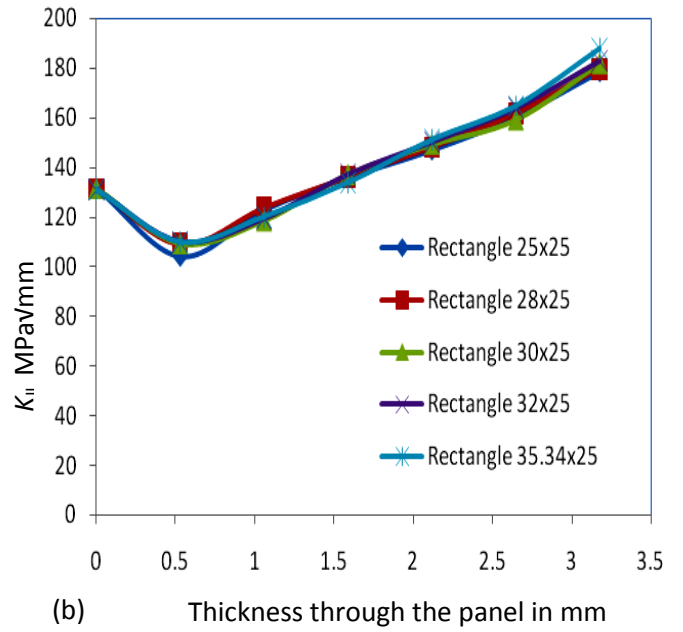
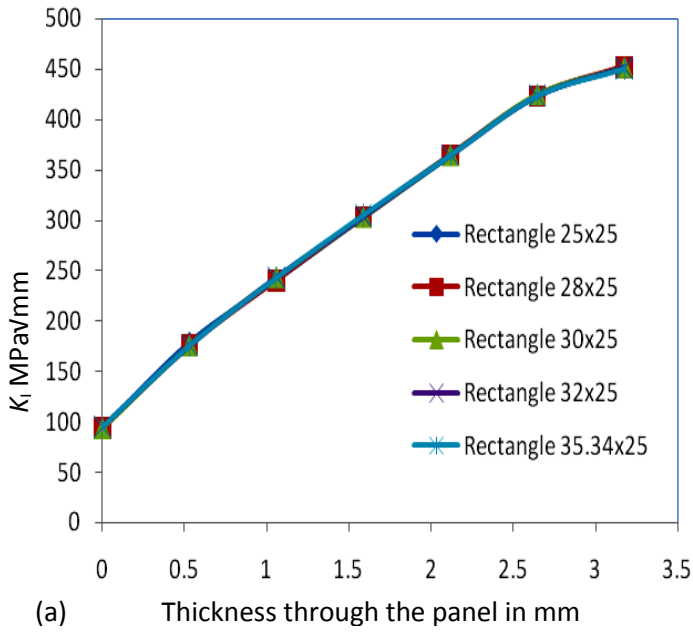


**Fig 4.2.** Variation of SIF through the thickness for rectangular patch applied on 30 degree crack (a)  $K_I$  (b)  $K_{II}$

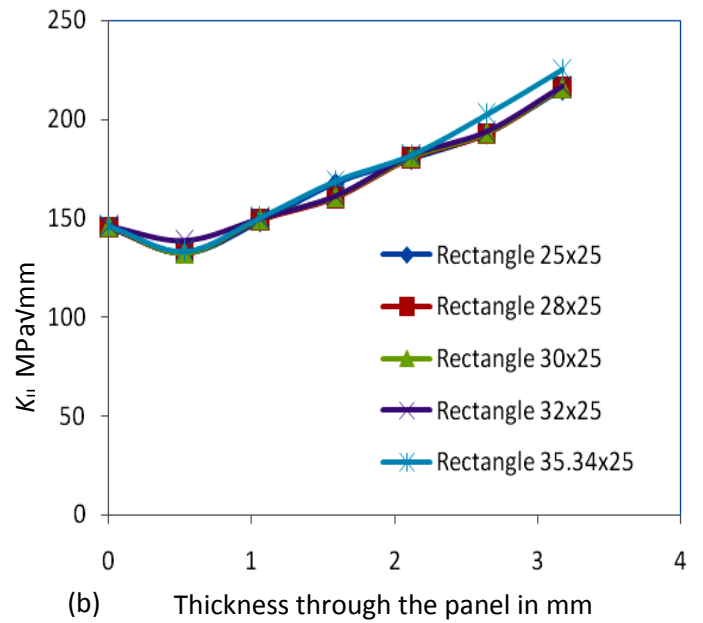
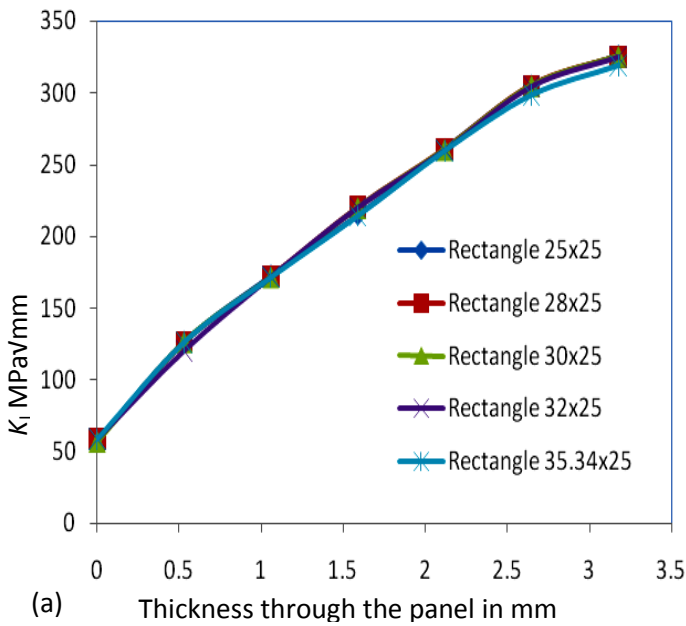
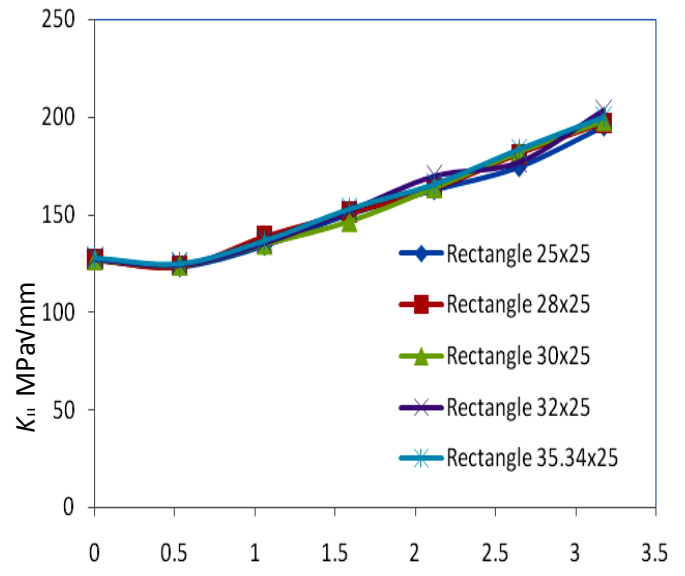
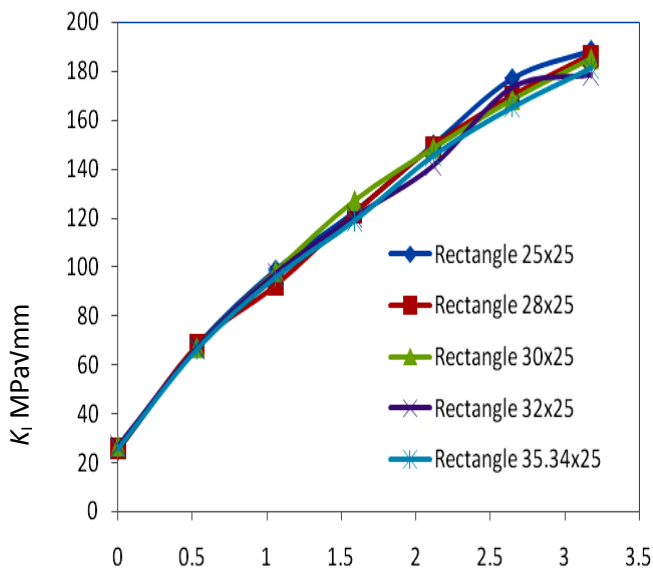


**Fig 4.3.** Variation of SIF through the thickness for rectangular patch for 45 degree crack (a)  $K_I$  (b)  $K_{II}$



(a) Thickness through the panel in mm  $K_I$  MPa√mm

(b) Thickness through the panel in mm  $K_{II}$  MPa√mm

**Fig 4.4.** Variation of SIF through the thickness for rectangular patch for a 60 degree crack (a)  $K_I$  (b)  $K_{II}$

#### 4.4 Unbalanced Laminates

The ply orientation of the composite laminates is one of the most important parameters in composite patch repair. For the double sided repair, we used unidirectional laminates to give reinforcement to the panel in the loading direction. In practical applications, it is desirable a small number of laminates be aligned perpendicular to lading direction to take in bi-axial loads. In single sided repair, the laminates also need to resist bending of the panel. Compared to unidirectional laminates, the unbalanced laminates produce a counter bending effect, hence resisting the bending. In this work, various unbalanced ply orientations have been tried for the single sided repair. One set of orientations were such that the ply angles were along and perpendicular to the loading direction and in another set the orientations were along and perpendicular to the crack.

It was shown that the shape of the patch has no effect on the repair. Hence we use only one shape which is the rectangle. The different crack inclination angles were 30, 45 and 60 degree.

For modelling the unbalanced laminates, we need to create a local coordinate system depending on the direction the fibres need to be aligned. Then each layer of the patch is selected and assigned the appropriate local coordinate system.

#### **4.5 Unbalanced laminates applied to 30 Degree crack**

The 30 degree crack has the largest component of the applied load perpendicular to the crack front. Hence the patching is primarily intended to reduce mode-I SIF. The analysis is done for different ply-angles ( $[0_2/ 30_2]$ ,  $[0_2/ 90_2]$ ,  $[30_2/ 0_2]$ ,  $[90_2/ 0_2]$ ,  $[30_4]$ ,  $[150_4]$ ,  $[30_2/ 150_2]$ ,  $[150_2/ 30_2]$ ,  $[150_4]$  and  $[90]_4$ ).  $[90]_4$  is considered since it offers highest resistance in the loading direction. Since the crack is mixed-mode, the load on the crack front will have components along and perpendicular to loading direction. For this reason  $[90_2/ 0_2]$  and  $[0_2/ 90_2]$  is used. Also since the load can also be considered having components along the crack front and perpendicular to it,  $[30_2/ 150_2]$ ,  $[150_2/ 30_2]$  laminate configuration is considered. From the Figures 4.5, 4.6, 4.7, and 4.8, we can see that  $[90_4]$  patch fiber configuration gives least SIF in mode I and there is not much difference between  $[90_4]$  and  $[0_2/90_2]$ . In mode II, The layup  $[0_2/90_2]$  is best suited. Overall, one can say the that  $[0_2/90_2]$  is the best layup because it gives the least SIF values and in case of slight bi-axial loads, the patch can take it. The layups with fibers aligned or perpendicular to the crack is not the optimum layup for 30 degree crack. The patch area does not influence the SIF values.

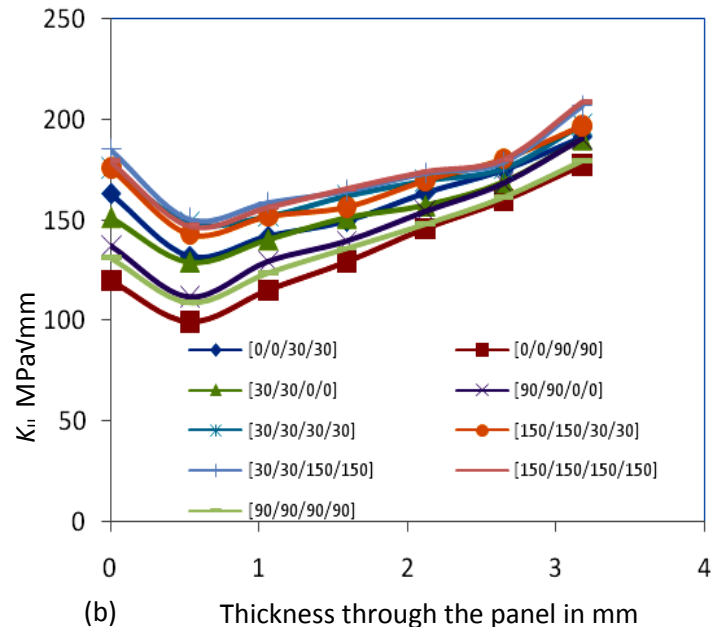
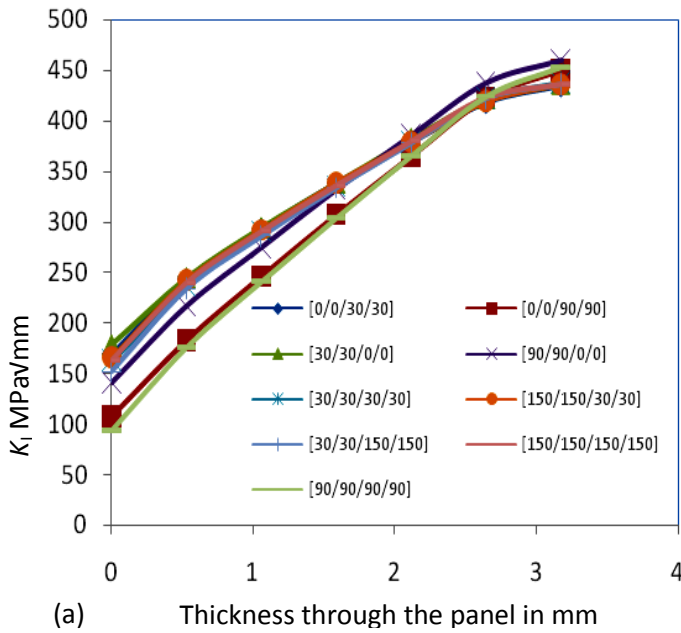


**Fig 4.5.** Variation of SIF through the thickness for rectangular patch of size 28x25 mm<sup>2</sup> for 30 degree crack (a)  $K_I$  (b)  $K_{II}$

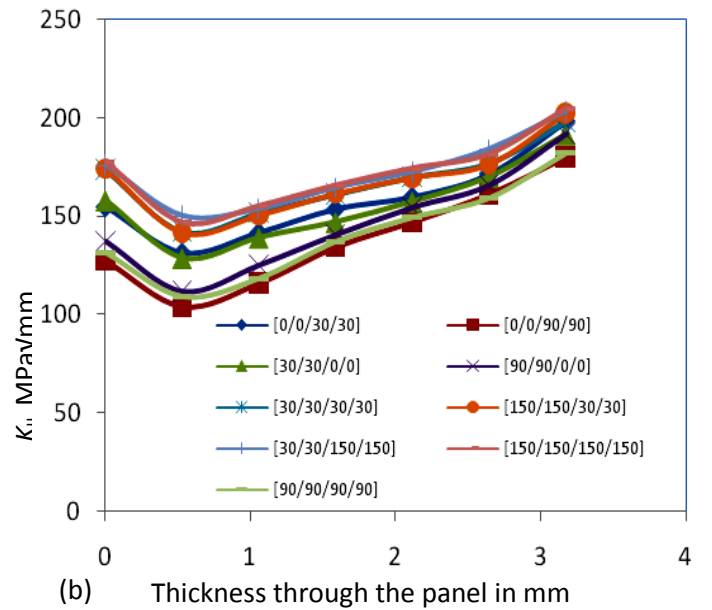
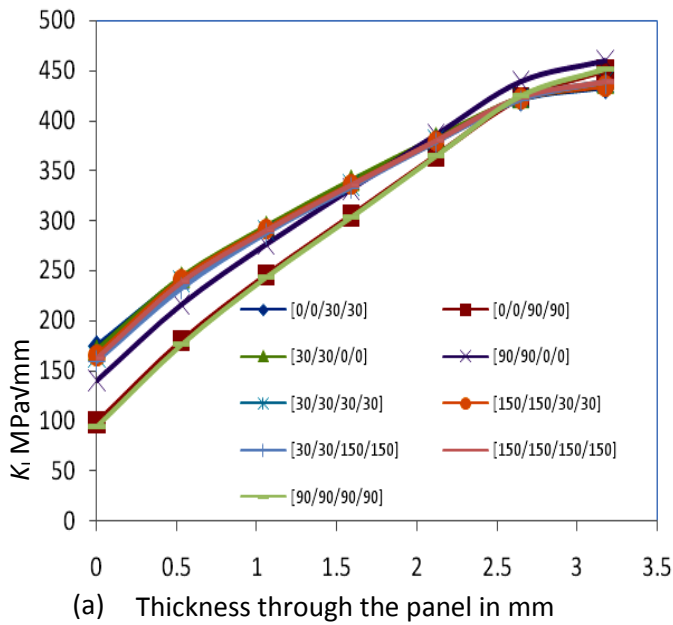


**Fig 4.6.** Variation of SIF through the thickness for rectangular patch of size 30x25 mm<sup>2</sup> for 30 degree crack (a)  $K_I$  (b)  $K_{II}$

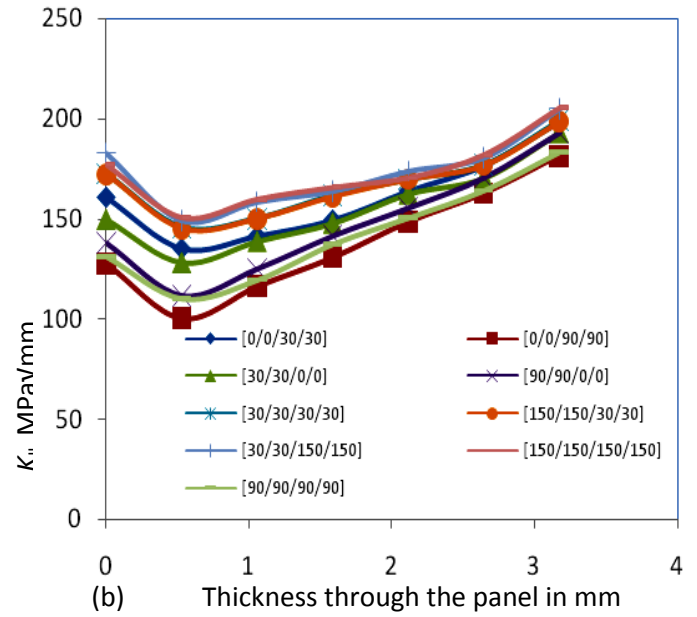
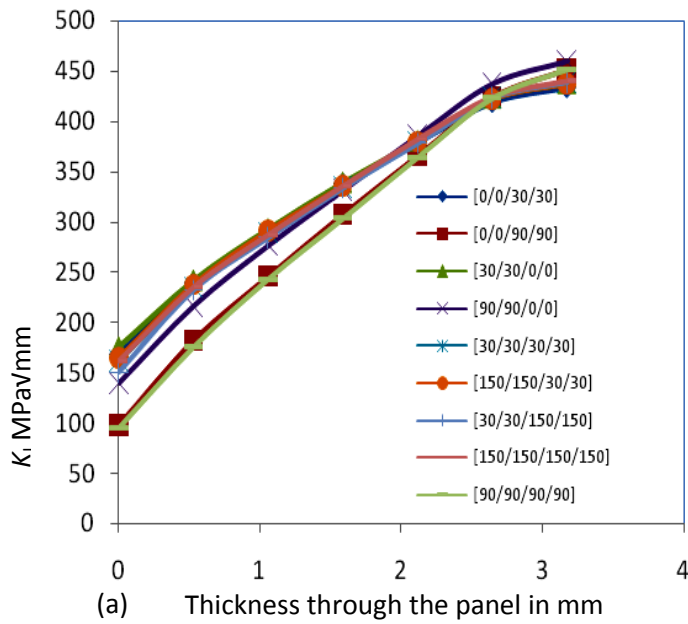


**Fig 4.7.** Variation of SIF through the thickness for rectangular patch of size  $32 \times 25 \text{ mm}^2$  for 30 degree crack (a)  $K_I$  (b)  $K_{II}$

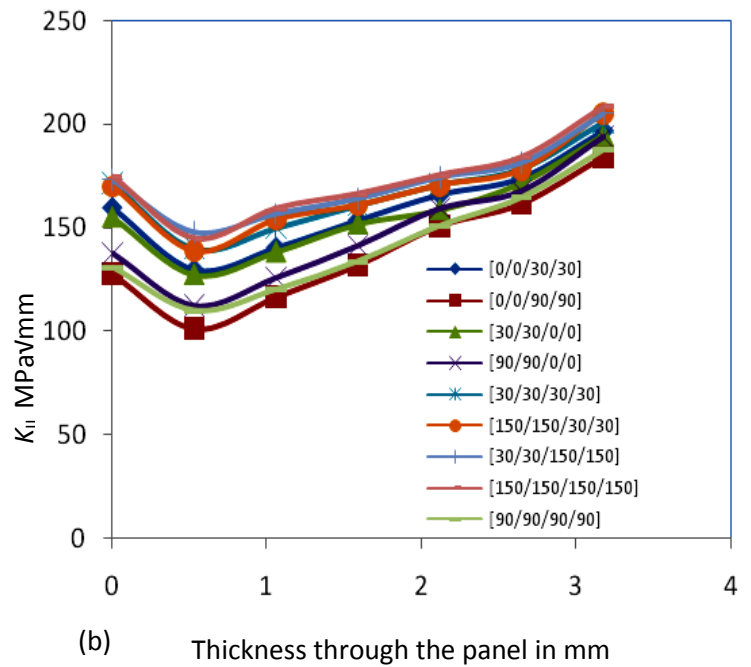
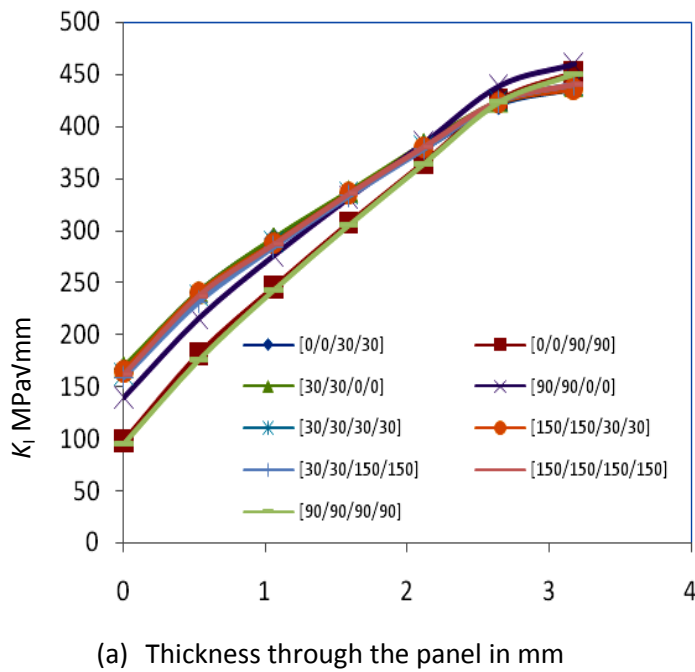


**Fig 4.8.** Variation of SIF through the thickness for rectangular patch of size  $35.36 \times 28 \text{ mm}^2$  for 30 degree crack (a)  $K_I$  (b)  $K_{II}$

#### 4.6 Unbalanced laminates applied to 45 Degree crack

The 45 degree crack has the components of the applied load perpendicular to the crack front and along it. The analysis is done for different ply-angles ( $[0_2/45_2]$ ,  $[0_2/90_2]$ ,  $[45_2/0_2]$ ,  $[90_2/0_2]$ ,  $[45_4]$ ,  $[135_4]$ ,  $[45_2/135_2]$ ,  $[135_2/45_2]$ ,  $[135_4]$  and  $[90_4]$ ).  $[90_4]$  is considered since it offers highest resistance in the loading direction. Since the crack is mixed-mode, the load on the crack front will have components along and perpendicular to loading direction. For this reason  $[90_2/0_2]$  and  $[0_2/90_2]$  is used. Also since the load can also be considered having components along the crack front and perpendicular to it,  $[45_2/135_2]$ ,  $[135_2/45_2]$  laminate configuration is considered. The impact of the ply orientation on the 45 degree patch was similar to that of 30 degree crack. From the Figures 4.9, 4.10, 4.11, and 4.12, we can see that  $[90_4]$  patch fiber configuration gives least SIF in mode I and there is not much difference between  $[90_4]$  and  $[0_2/90_2]$ . In mode II, The layup  $[0_2/90_2]$  is best suited. Overall, one can say that  $[0_2/90_2]$  is the best layup because it gives the least SIF values and in case of slight bi-axial loads, the patch can take it. The layups with fibers aligned or perpendicular to the crack is not the optimum layup for 45 degree crack. Different patch shape does not influence the SIF values.

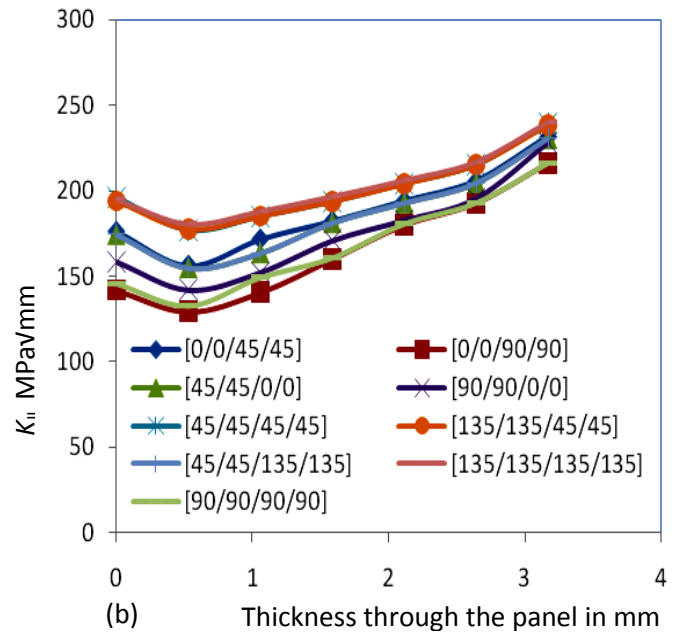
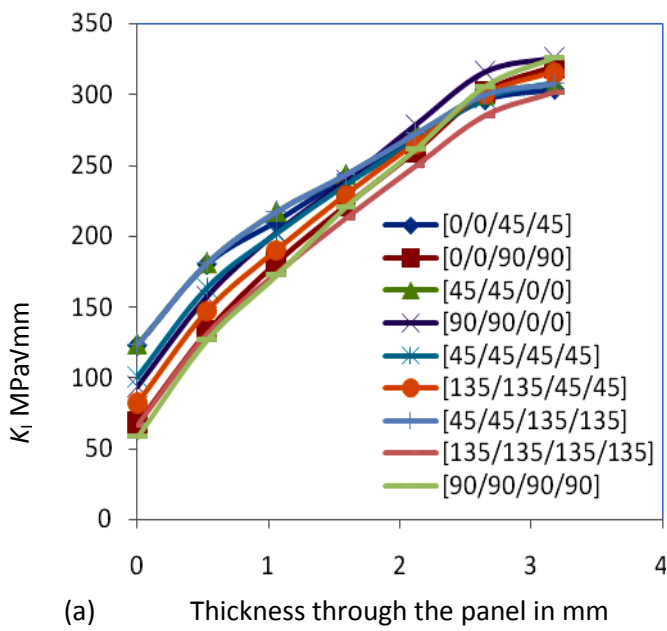


**Fig 4.9.** Variation of SIF through the thickness for rectangular patch of size 28x25 mm<sup>2</sup> for 45 degree crack (a)  $K_I$  (b)  $K_{II}$

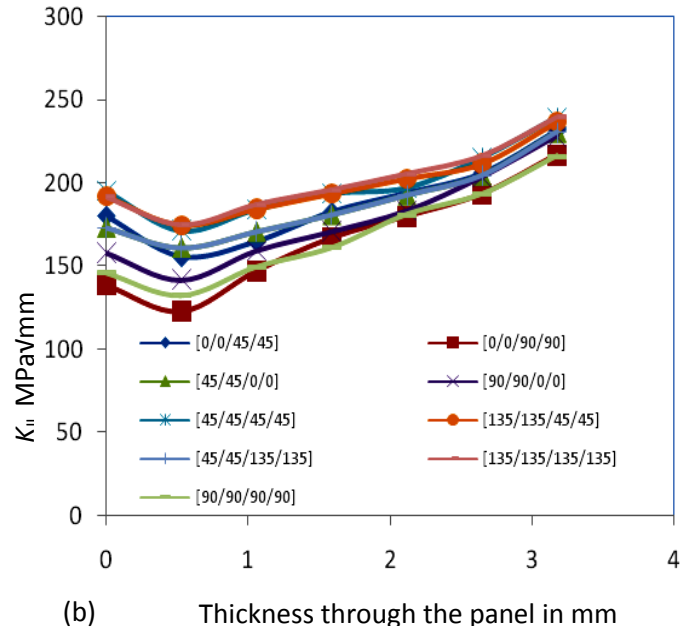
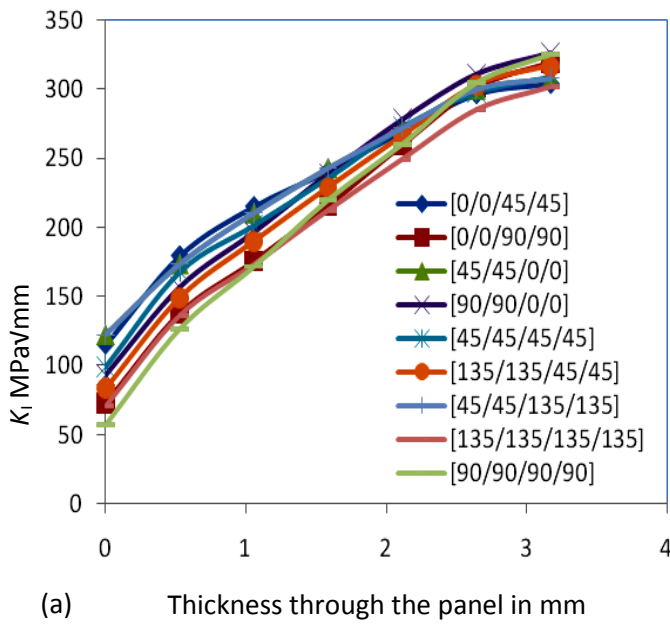


**Fig 4.10.** Variation of SIF through the thickness for rectangular patch of size 30x25 mm<sup>2</sup> for 45 degree crack (a)  $K_I$  (b)  $K_{II}$



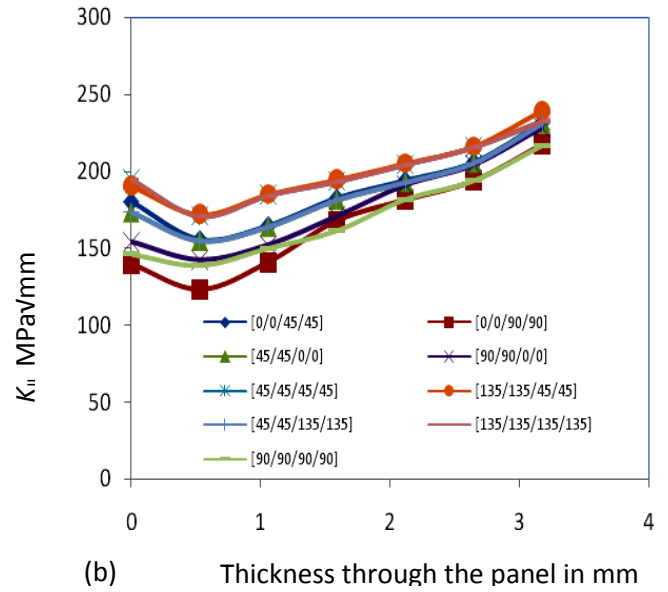
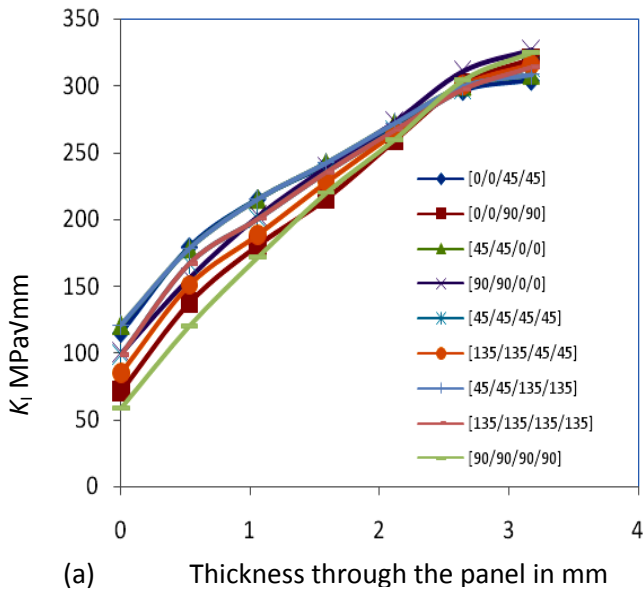


**Fig 4.11.** Variation of SIF through the thickness for rectangular patch of size 32x25 mm<sup>2</sup> for 45 degree crack (a)  $K_I$  (b)  $K_{II}$

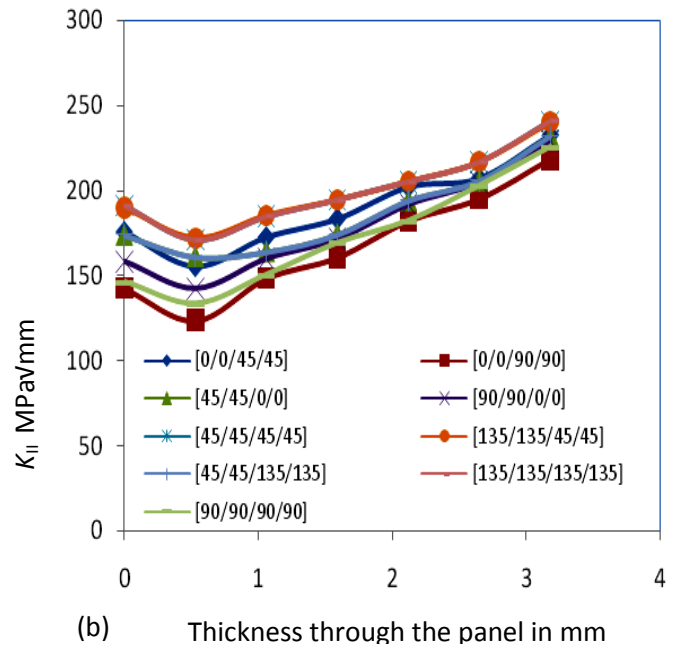
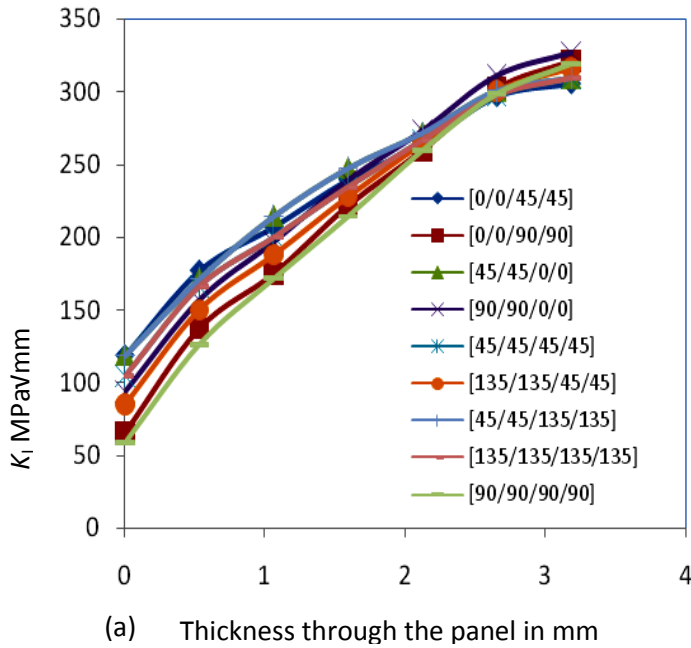


**Fig 4.12.** Variation of SIF through the thickness for rectangular patch of size 35.36x25 mm<sup>2</sup> for 45 degree crack (a)  $K_I$  (b)  $K_{II}$

### 4.7 Unbalanced laminates applied to 60 Degree crack

The 60 degree crack has the components of the applied load perpendicular to the crack front and along it. The component of stress along the crack front is greater than the one perpendicular to it. The analysis is done for different ply-angles ( $[0_2/ 60_2]$ ,  $[0_2/ 90_2]$ ,  $[60_2/ 0_2]$ ,  $[90_2/ 0_2]$ ,  $[60_4]$ ,  $[120_4]$ ,  $[60_2/ 120_2]$ ,  $[120_2/ 60_2]$ ,  $[135_4]$  and  $[90_4]$ ).  $[90_4]$  is considered since it offers highest resistance in the loading direction. Since the crack is mixed-mode, the load on the crack front will have components along and perpendicular to loading direction. For this reason  $[90_2/ 0_2]$  and  $[0_2/ 90_2]$  is used. Also since the load can also be considered having components along the crack front and perpendicular to it,  $[45_2/ 135_2]$ ,  $[135_2/ 45_2]$  laminate configuration is considered. The impact of the ply orientation on the 60 degree patch was similar to that of 45 degree crack. From the Figures 4.13, 4.14, 4.15, and 4.16, we can see that  $[90_4]$  patch fiber configuration does not give least SIF in mode I as in previous cases. The  $[120_4]$  gives the best ply layout in mode-I SIF. Overall, one can say that  $[120_4]$  is the best layup because it gives the least SIF values and in case of slight bi-axial loads, the patch can take it.

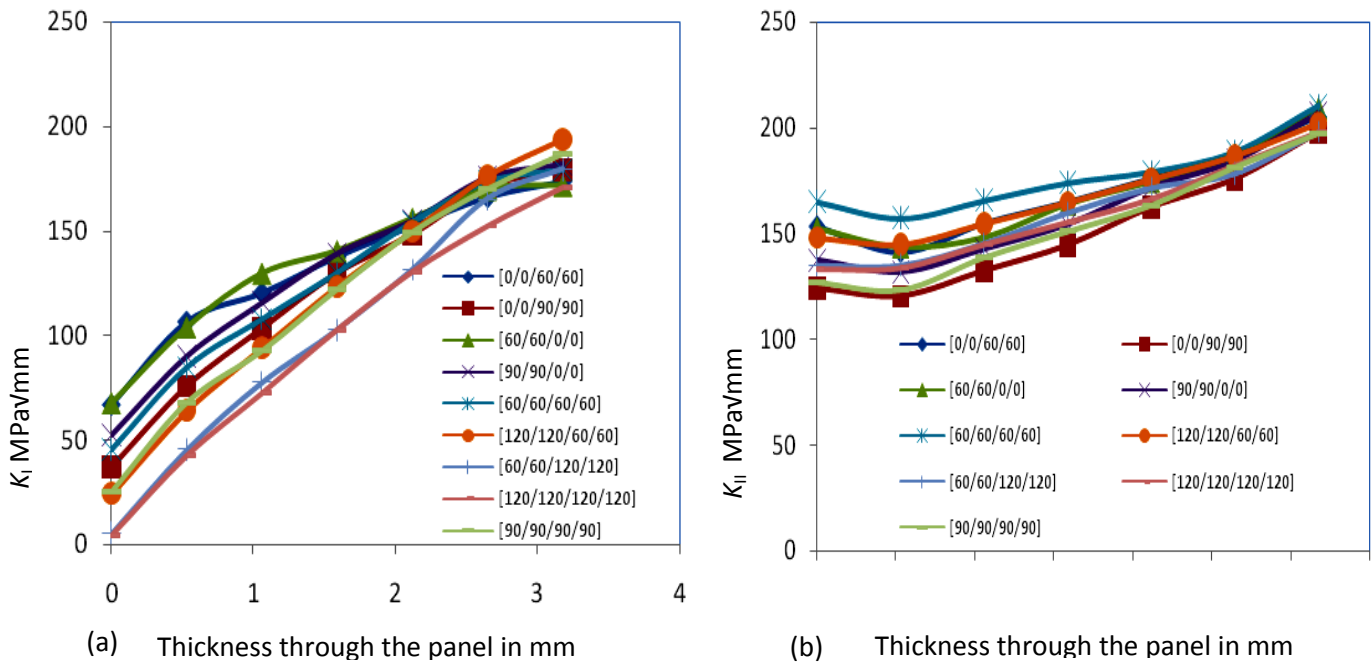


**Fig 4.13.** Variation of SIF through the thickness for rectangular patch of size 35.36x25 mm<sup>2</sup> for 60 degree crack (a)  $K_I$  (b)  $K_{II}$

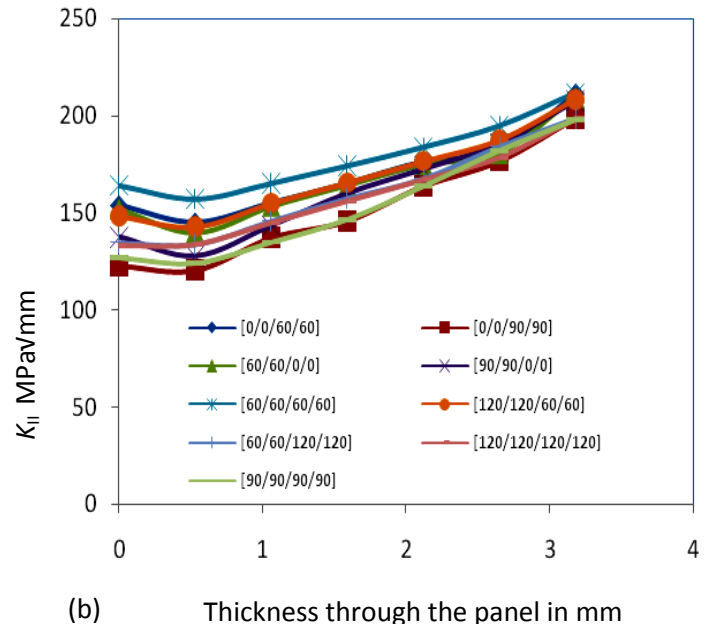
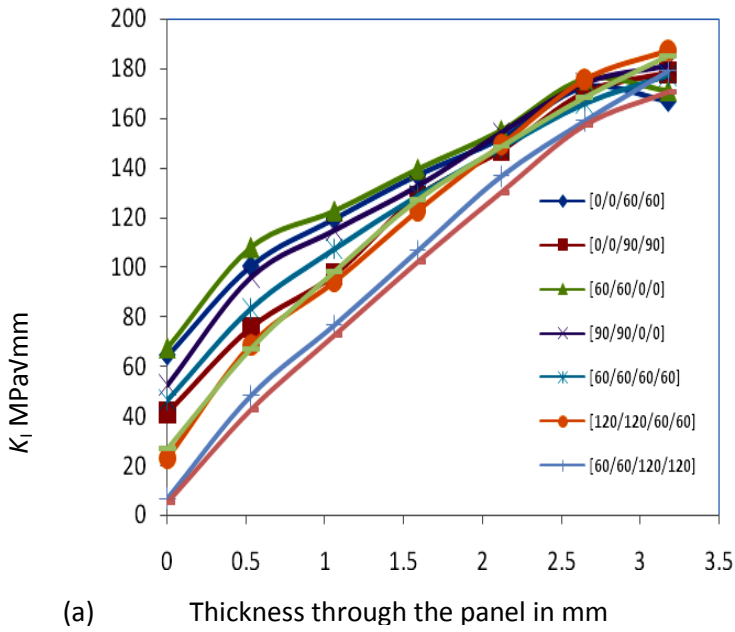


**Fig 4.14.** Variation of SIF through the thickness for rectangular patch of size 30x25 mm<sup>2</sup> for 60 degree crack (a)  $K_I$  (b)  $K_{II}$

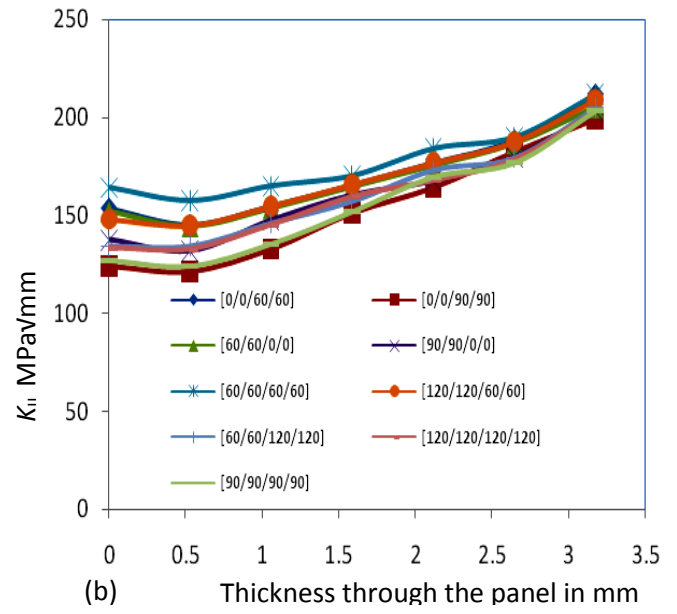
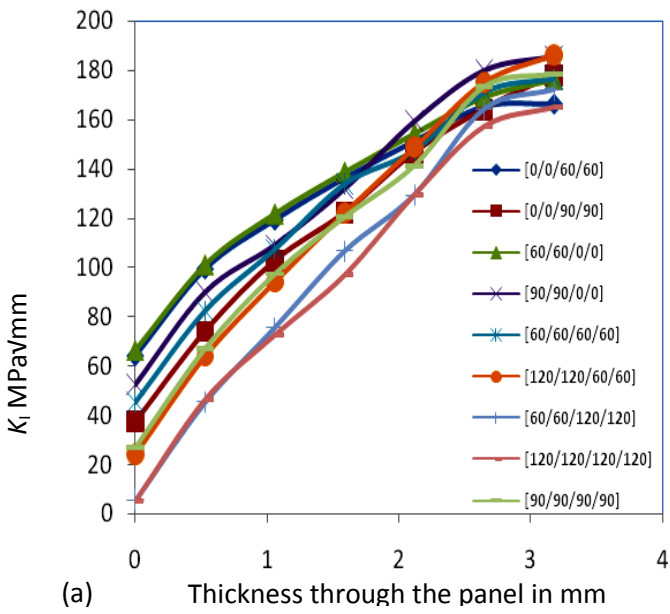


**Fig 4.15.** Variation of SIF through the thickness for rectangular patch of size 32x25 mm<sup>2</sup> for 60 degree crack (a)  $K_I$  (b)  $K_{II}$

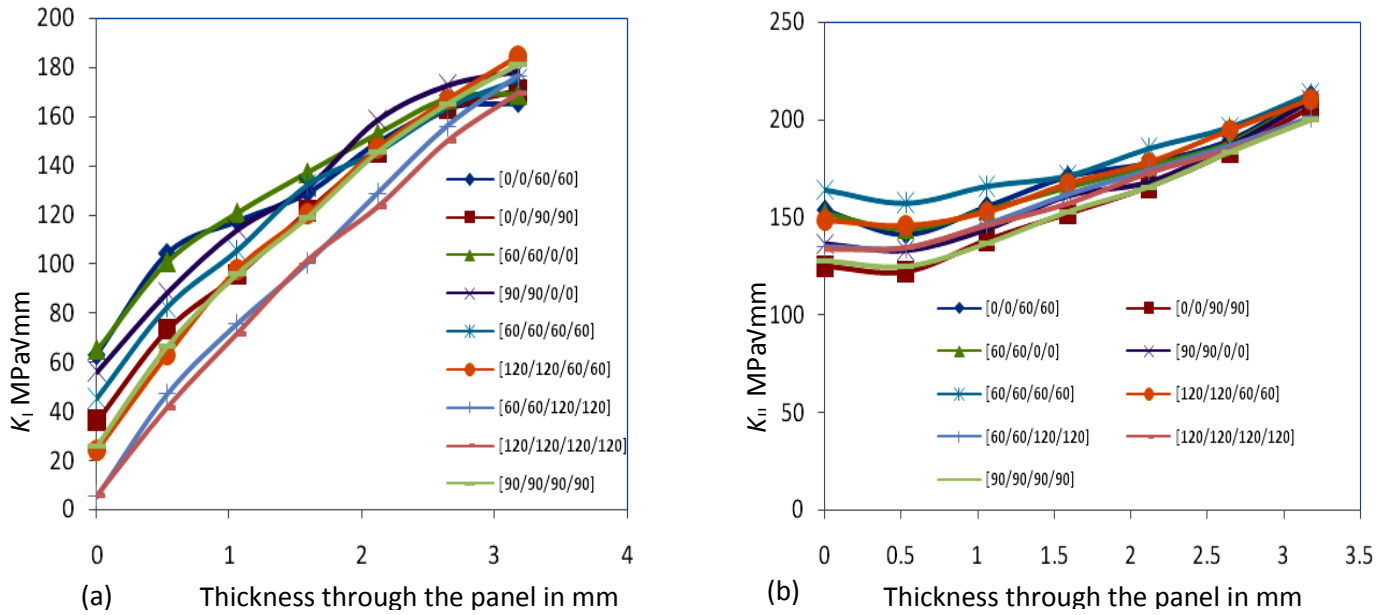


**Fig 4.16.** Variation of SIF through the thickness for rectangular patch of size 35.36x25 mm<sup>2</sup> for 60 degree crack (a)  $K_I$  (b)  $K_{II}$

#### 4.8 Comparison of [90<sub>4</sub>] and [0<sub>2</sub>/ 90<sub>2</sub>] applied to different mixed mode cracks

From the figures 4.17 and 4.18, for a given ply angles sequence, we can see that  $K_I$  is maximum for the crack inclination angle of 30 degree and minimum for 60 degree. However for  $K_{II}$  we can see that it is maximum for 45 degree instead of 60 degree. This is because there is very little opening of the crack when crack inclination angle is 60 degrees as loading almost aligns along the crack. One can say it is better to use [90<sub>4</sub>] because in case of unbalanced laminates, there is a chance of debonding of the laminates from the composites.

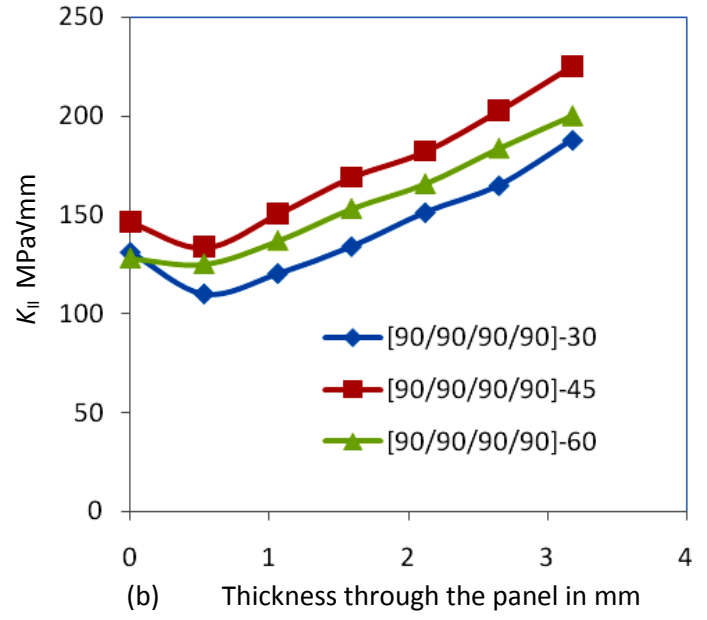
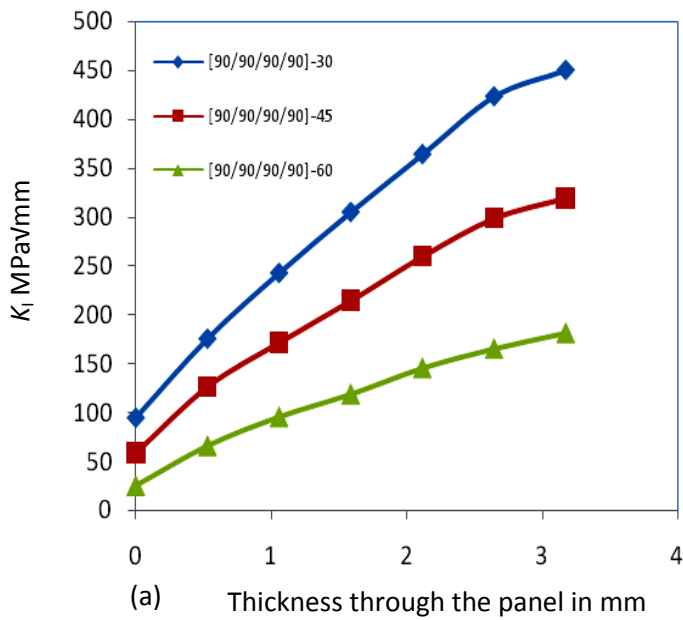


**Fig 4.17.** Variation of SIF through the thickness for of different crack inclination angles for rectangular patch of size 35.36x25 mm<sup>2</sup> for patch lay-up [90<sub>4</sub>] (a)  $K_I$  (b)  $K_{II}$

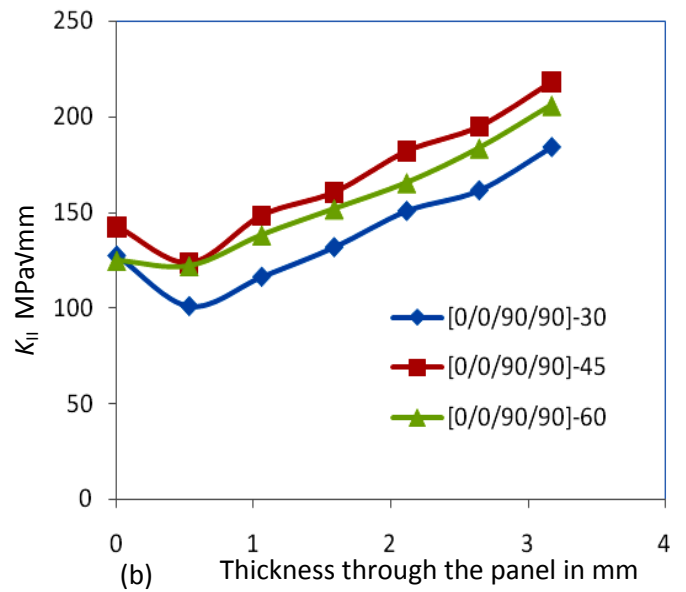
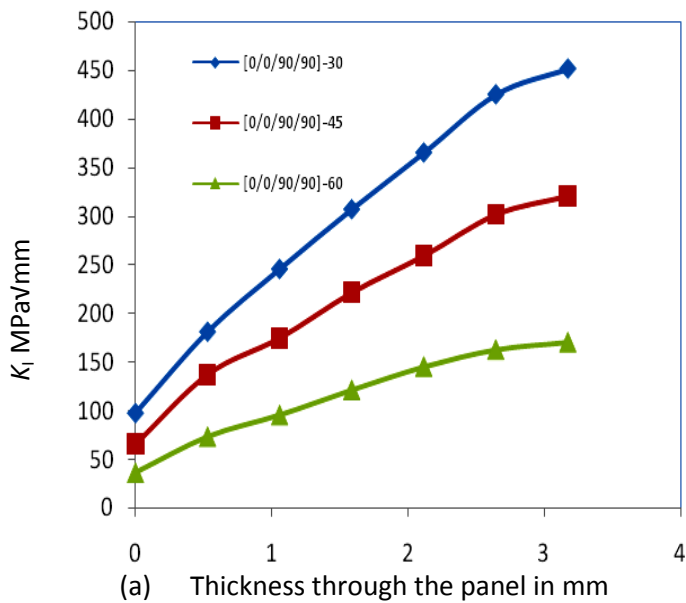


**Fig 4.18.** Variation of SIF through the thickness for of different crack inclination angles for rectangular patch of size 35.36x25 mm<sup>2</sup> for patch lay-up [90<sub>2</sub> | 0<sub>2</sub>] (a)  $K_I$  (b)  $K_{II}$

## 4.9 Transversely graded materials

Transversely graded materials are those in which the Young's modulus varies through the thickness of the material. However, the Poisson's ratio remains the same through the thickness. In the plane of the panel, the material has no property variation, but the material is formed by binding materials of different Young's modulus. In the present work, the graded material is the patch. Since there is not much impact of the patch on the patch for single-sided repair, we use a transversely graded patch. The patch consists of 14 layers of isotropic material whose  $E$  varies from 200 MPa to 250 MPa (Figure 4.19). The analysis is done for the rectangular and circular patch for crack inclination angles of 30, 45 and 60 degrees.

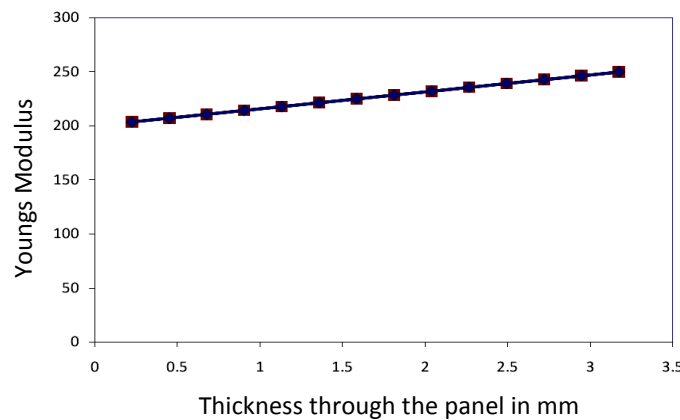
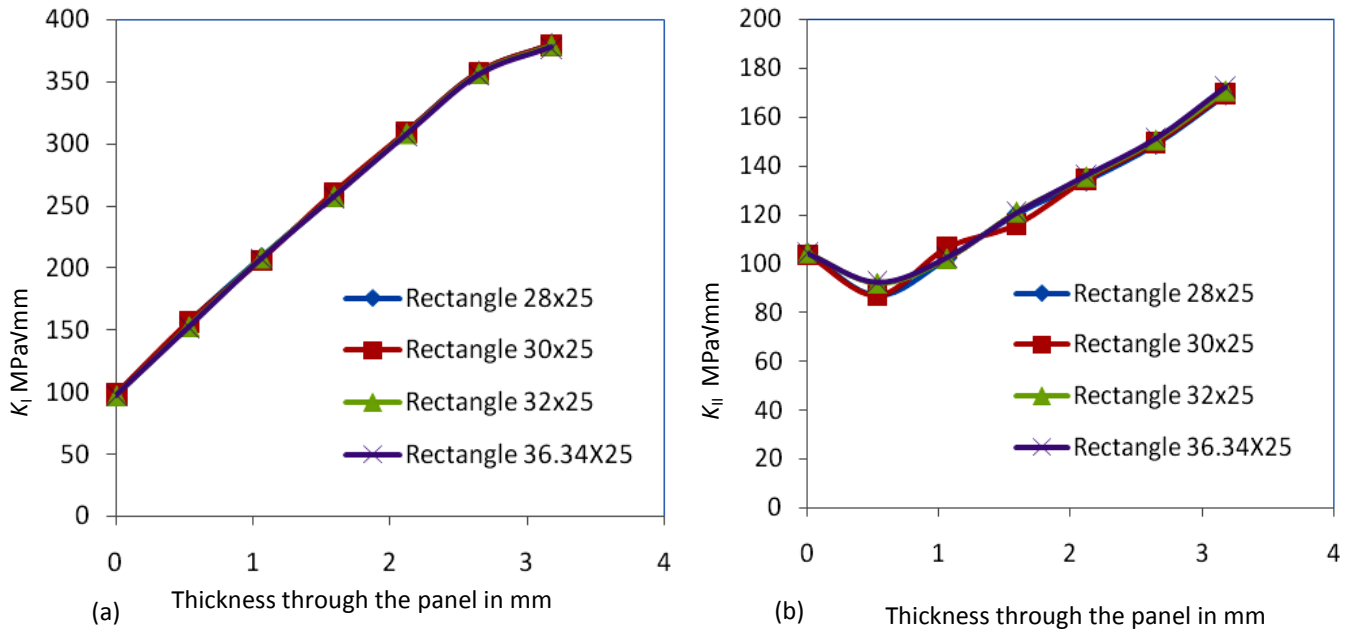


Fig4.19. Variation of  $E$  through the thickness of patch

## 4.10 Transversely graded material applied to different mixed-mode cracks

Transversely graded patch was applied to different mixed mode cracks. The patch shape taken is rectangle. Other shapes were not considered as the patch shape has little impact on the given mixed-mode crack. From figures 4.20, 4.21 and 4.22, it is seen that for the transversely graded material the patch geometry does not influence the SIF values. These SIF values are slightly lower than the composite patches. For a panel with a 30 degree crack, the  $K_I$  value after repair is higher compared to 45 and 60 degree cracks. For the panel with 45 degree crack,  $K_{II}$  after repair is higher than 30 and 60 degree cracked panels.



**Fig 4.20.** Variation of SIF through the thickness for single sided rectangular patch for 30 degree crack using transversely graded patch (a)  $K_I$  (b)  $K_{II}$

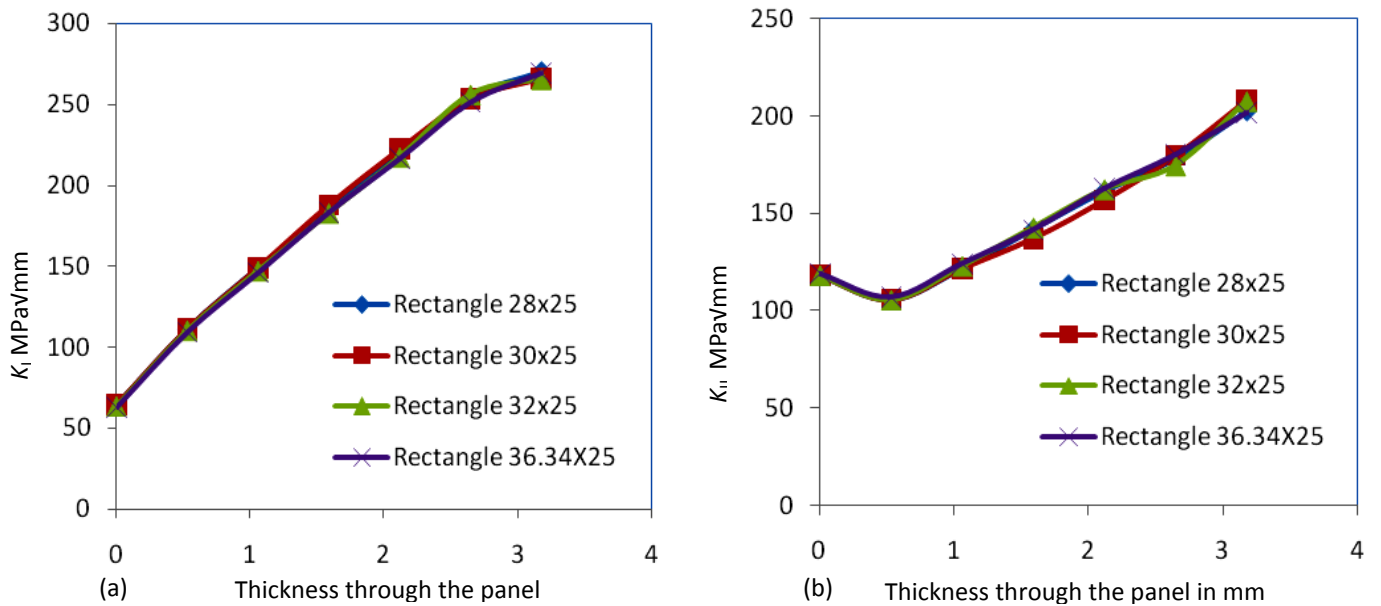


**Fig4.21.** Variation of SIF through the thickness for single sided rectangular patch for 45 degree crack using transversely graded patch (a)  $K_I$  (b)  $K_{II}$

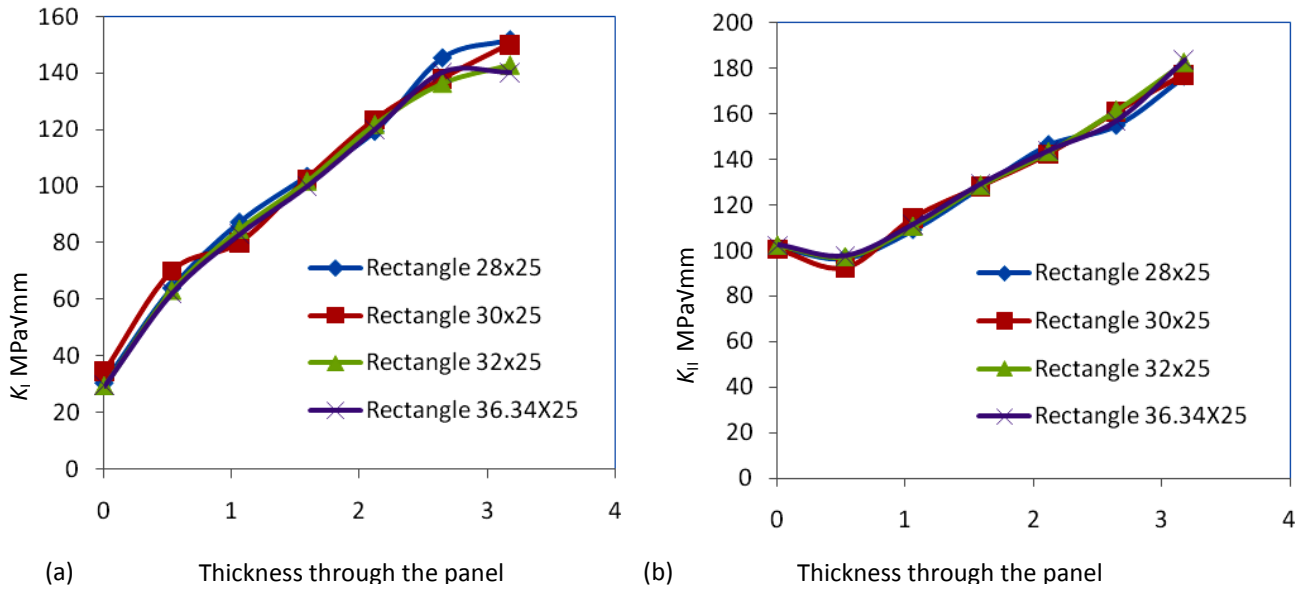


**Fig 4.22.** Variation of SIF through the thickness for single sided rectangular patch for 60 degree crack using transversely graded patch (a)  $K_I$  (b)  $K_{II}$

#### 4.11 Closure

It is seen that the SIF values after repair does not vary significantly with different patch geometry. For the 60 degree crack, the  $K_{II}$  values after repair is lower than the 45 degree crack.  $K_I$  for the 60 degree crack is lower than 30 degree and 45 degree crack. For the 30 and 45 degree cracks, the patch layup configuration of  $[0_2/90_2]$  gives optimum reduction in the SIF values. However because of the deboning effects in using the unbalanced laminates,  $[90_4]$  is preferred. For the 60 degree crack,  $[120_4]$  is the optimum layup configuration. The transversely graded materials showed the best reduction in SIF values compared to unbalanced laminates and it doesn't debond on  $[0_290_2]$  configuration. Hence transversely graded material for patch is preferred.



# Chapter 5

## Conclusion and Recommendations for Future Work

The behaviour of double sided composite repair is completely different from the single sided repair. In case of double sided repair circular patch seems to be optimum for reducing both  $K_I$  and  $K_{II}$ . In case of single sided repair, irrespective of the patch shape, the behaviour is one and the same. This is because of the additional bending it undergoes due to neutral axis shift. Also SIF reduction is effective for unbalanced lay-up configuration. As the fibres are not oriented parallel to load direction, it debonds during fatigue loading. Hence patch made of transversely graded material is recommended for the first time in literature and it proved effective in SIF reduction ( $K_I$ ) at un-patched surface.

The present work deals with the effect of a patch of thickness of 1.5 mm. More study can be done for different patch thickness. The work can be extended to study the effect of other patch parameters like the patch thickness, patch perimeter. Another interesting aspect of composite patch repair is the effect of tapered patch. In case of single sided patch one can see bending of panel due to shift in neutral axis. But in reality, the length of the wing is much longer than dimension of the patch. Actual behavior can be different if actual size effect is considered. Therefore it can be extended to study the composite patch repair effect on very large panel dimensions. Also the effect of SIF on different crack lengths and crack inclination angles can be studied. In practice, the aircraft is subjected to a wide range of temperatures. Hence thermo-mechanical study of bonded repaired panel can be carried out. Further in this work we consider that energy release rate is contributed by mode-I and mode-II fracture. But mode-III component exists especially in the case of single sided repaired panel. Variation on  $K_{III}$  would be of particular interest in fatigue life estimation. In this study only linear fracture mechanics is considered but in practice fracture is associated with non-linear fracture

mechanics where plastic effect is considered around the crack tip. Thus the non linear effect can be included. The present work is carried out using boron/Epoxy laminates which is not easily available. Carbon/Epoxy laminate being widely available need to be studied. It is assumed in this work that the crack does not propogate to the composite. In reality this is a possibility and it would be very challenging to study as very little work has been done in this aspect.

# References

- [1] A. A. Baker and R. Jones., Bonded repair of aircraft structures. Dordrecht, Netherlands, Martinus Nijhoff Publisher, 1988.
- [2] <http://www.dsto.defence.gov.au/research/5598/>
- [3] M. D. Coffin and C. F. Tiffany, "New Air Force Requirements for Structural Safety, Durability, and Life Management" AIAA Journal of Aircraft, volume13, 1976.
- [4] A.A.Baker, "A summary of work on applications of advanced fibre composites at the Aeronautical Research Laboratories" Composites, 9:11-16, January 1978
- [5] R. Jones, R.J. Callinan "A crack opening displacement approach to crack patching" Engineering Fracture Mechanics, 13:801-806, 1980
- [6] R. Jones, R.J. Callinan, K.C. Aggarwal, "Analysis of bonded repairs to damaged fibre composite structures" Engineering Fracture Mechanics, 17:37-46, 1983
- [7] Ramesh Chandra, M.V.V. Murthy, T.S. Ramamurthy, A.K. Rao, "Analytical estimation of stress intensity factors in patched cracked plates" Engineering Fracture Mechanics, 21: 479-494, 1985
- [8] R. Sethuraman, S.K. Maiti, "Determination of mixed mode stress intensity factors for a crack-stiffened panel", Engineering Fracture Mechanics, 33:355-369, 1989
- [9] R. Sethuraman, S.K. Maiti, "Finite element analysis of doubly bonded crack-stiffened panels under mode I or mode II loading" Engineering Fracture Mechanics, 34:465-475, 1989
- [10] Ching-Hwei Chue, Li-Chung Chang, Jang-Shing Tsai "Bonded repair of a plate with inclined central crack under biaxial loading" Composite Structures, 28:39-45, 1994
- [11] Ching-Hwei Chue, Thomas Jin-Chee Liu "The effects of laminated composite patch with different stacking sequences on bonded repair" Composites Engineering, 5:223-230, 1995
- [12] T. E. Tay, F. S. Chau, C. J. Er, "Bonded boron-epoxy composite repair and reinforcement of cracked aluminium structures" Composite Structures, 34:339-347, 1996
- [13] Chorng-Fuh Liu, Horng-Shian Jou, Ying-Te Lee, "Stress intensity factor of a patched crack", International Journal of Solids and Structures, 34:1557-1562, 1997
- [14] J. C. Klug, C. T. Sun, "Large deflection effects of cracked aluminum plates repaired with bonded composite patches" Composite Structures, 42:291-296, 1998

- [15] M. L. Scott, J. A. S. Raju, A. K. H. Cheung, "Design and manufacture of a post-buckling co-cured composite aileron" *Composites Science and Technology*, 58:199-210, 1998
- [16] Turaga V.R.S. Umamaheswar, Ripudaman Singh, "Modelling of a patch repair to a thin cracked sheet", *Engineering Fracture Mechanics*, 62:267-289, 1999
- [17] A. Mahadesh Kumar, S.A. Hakeem, "Optimum design of symmetric composite patch repair to centrec racked metallic sheet", *Composite Structures* 49:285-292, 2000
- [18] B. Bachir Bouiadjra, M. Belhouari, B. Serier, "Computation of the stress intensity factors for repaired cracks with bonded composite patch in mode I and mixed mode", *Composite Structures* 56:401–406, 2002
- [19] Dae-Cheol Seo, Jung-Ju Lee, "Fatigue crack growth behavior of cracked aluminum plate repaired with composite patch", *Composite Structures* 57:323–330, 2002
- [20] Q. Y. Wang, R. M. Pidaparti, "Static characteristics and fatigue behavior of composite-repaired aluminum plates" *Composite Structures*, 56:151-155, 2002
- [21] Ki Hyun Chung , Won H Yang , "Mixed mode fatigue crack growth in aluminum plates with composite patches" *International Journal of Fatigue*, 25:325-333, 2003
- [22] Jean-Denis Mathias, Xavier Balandraud, Michel Grediac, "Applying a genetic algorithm to the optimization of composite patches" *Computers & Structures*, 84:823-83, 2006
- [23] H. Hosseini-Toudeshky, B. Mohammadi, S. Bakhshandeh, "Mixed-mode fracture analysis of aluminium repaired panels using composite patches", *Composites Science and Technology* 66:188–198, 2006
- [24] H. Hosseini-Toudeshky, B. Mohammadi and S. Bakhshandeh, "Mixed-mode fatigue crack growth of thin aluminium panels with single-side repair using experimental and numerical methods", *Fatigue Fract Engng Mater Struct* , 30:629–639, 2007
- [25] K. Madani S. Touzain, X. Feaugas, M. Benguediab and M. Ratwani, "Numerical analysis for the determination of the stress intensity factors and crack opening displacements in plates repaired with single and double composite patches", *Computational Materials Science* 42:385–393, 2008
- [26] J.R Rice, "A path independent integral and the approximation analysis of strain concentration by notches and cracks" *Journal of Applied Mechanics*, 35:379 – 386, 1968
- [27] C.F Shih, Moran, B. Nakamura, "T. Energy release rate along a three dimensional crack front in a thermally stressed body", *International Journal of Fracture*, 30: 79 – 102, 1986
- [28] Prashant Kumar, *Elements of Fracture Mechanics*, Tata McGraw Hill Publishing Co. Ltd, New Delhi, 2009

## **List of the papers submitted on the basis of this thesis**

1. M.Ramji, R Srilakshmi and Bhanu Prakash M, "Towards an optimum patch in composite patch repair", Proc. International Conference on Theoretical, Applied, Computational, Experimental Mechanics ( ICTACEM-2010), IIT Kharagpur, 27<sup>th</sup> – 29<sup>th</sup> December, 2010.
2. Bhanu Prakash M and M Ramji, "Optimum patch design in composite repair for mixed-mode loading", Proc. International Conference on Computational Methods in Manufacturing (ICMM 2011), IIT Guwahati